

1 **Using Inertial Measurement Units originally developed for biomechanics for modal testing of**  
2 **civil engineering structures**

3 David Hester<sup>a</sup>, James Brownjohn<sup>b</sup>, Mateusz Bocian<sup>c</sup>, Yan Xu<sup>b</sup>, Antonino Quattrone<sup>d</sup>

4 <sup>a</sup>School of Natural and Built Environment, Queen's University Belfast, UK

5 <sup>b</sup>Vibration Engineering Section, University of Exeter, UK

6 <sup>c</sup>Department of Engineering, University of Leicester, UK

7 <sup>d</sup>Civil and Construction Engineering, Politecnico di Torino, Italy  
8

9 **Abstract**

10 This paper explores the use of wireless Inertial Measurement Units (IMU) originally developed for  
11 bio-mechanical research applications for modal testing of civil engineering infrastructure. Due to  
12 their biomechanics origin, these devices combine a triaxial accelerometer with gyroscopes and  
13 magnetometers for orientation, as well as on board data logging capability and wireless  
14 communication for optional data streaming and to coordinate synchronisation with other IMUs in a  
15 network. The motivation for application to civil structures is that their capabilities and simple  
16 operating procedures make them suitable for modal testing of many types of civil infrastructure of  
17 limited dimension including footbridges and floors while also enabling recovering of dynamic forces  
18 generated and applied to structures by moving humans. To explore their capabilities in civil  
19 applications, the IMUs are evaluated through modal tests on three different structures with  
20 increasing challenge of spatial and environmental complexity. These are, a full-scale floor mock-up in  
21 a laboratory, a short span road bridge and a seven story office tower. For each case, the results from  
22 the IMUs are compared with those from a conventional wired system to identify the limitations. The  
23 main conclusion is that the relatively high noise floor and limited communication range will not be a  
24 serious limitation in the great majority of typical civil modal test applications where convenient  
25 operation is a significant advantage over conventional wired systems.

26 **Keywords:** Operational Modal analysis; Wireless sensors; Ambient vibration; Civil engineering  
27 structures.

28 **1.0 Introduction**

29 The conventional view of civil infrastructure health monitoring is an array of permanently installed  
30 instrumentation with continuous data acquisition and data interpretation. Such structural health  
31 monitoring (SHM) systems are usually deployed on new landmark structures, with practically every  
32 new long suspended span bridge design including permanent instrumentation. There is an argument  
33 that such large structures will not benefit from SHM until they begin to age and that resources  
34 would be more effectively deployed on a larger number of smaller, older, but still critical  
35 infrastructure components such as the many masonry arch bridges and viaducts built in Victorian  
36 Britain. The large number of these older structures (e.g. tens of thousands of bridges in the UK) rule  
37 out comprehensive permanent monitoring, but there is a case for peripatetic monitoring systems for  
38 vibration and load testing. Such relocatable instrumentation arrays must be deployable easily and  
39 rapidly.

40 Short term instrumentation typically comprises strain gauges and/or accelerometers [1]. Strain  
41 gauges are primarily used for capturing static and quasi-static effects with accelerometers primarily  
42 capturing dynamic effects. In fact accelerometers are widely used for structural identification (St-id),  
43 which comprises system identification (modal analysis) designed to validate numerical models and  
44 to understand and predict dynamic performance [2]. Accelerometers deployed in civil infrastructure  
45 St-id applications have traditionally been large wired devices using piezo-electric sensing elements  
46 or servo-control of a proof mass. Requirements from a wide range of user communities have driven  
47 development of micro electrical mechanical system (MEMS) accelerometers that are small, light,  
48 inexpensive and low power. The potential to deploy MEMS accelerometers for civil infrastructure  
49 SHM applications has led to a large volume of research in smart wireless accelerometers for long-  
50 term deployment. Most such sensors have been designed and deployed by the research community,  
51 with exemplar applications such as the large scale Imote2 deployment on Jindo Bridge [3]. While  
52 most SHM research has gone on long term deployments of wireless sensors, few deployments focus  
53 on short term investigations [4]. Also, while there are many commercial solutions for wireless  
54 sensing of non-dynamic data there are fewer commercial wireless accelerometers. These are  
55 generally optimised applications such as in automotive and aerospace engineering where  
56 acceleration ranges are relatively large compared to the sub-1 g ranges experienced in operational  
57 monitoring of civil infrastructure such as bridges and buildings.

58

59 Accelerometers have been used in the biomechanics community for many years e.g. for gait analysis  
60 [5]. Inertial measurement units (IMUs) were developed with incorporation of gyroscopes [6] and  
61 magnetometers, and were subsequently available for wireless data acquisition [7]. Demand from the  
62 biomechanics community with applications in health and sport have driven development of  
63 commercial systems that are used in short term in-vivo instrumentation e.g. for hospital outpatient  
64 diagnosis, movement science experiments and for study and enhancement of sports performance.  
65 These systems both complement and replace optics-based motion capture systems and may be used  
66 with force plates and instrumented treadmills. The large rotations and translations involved require  
67 conversion to global (world) coordinate systems (WCS) but other than this, the requirements for  
68 size, weight, wireless communication and low power are remarkably similar to the requirements for  
69 vibration measurements of civil infrastructure. This was the experience of the authors when using  
70 biomechanics IMUs for tracking human movements in open space as part of research on vibration  
71 serviceability of footbridges [8].

72 Problematic footbridge vibrations occur at frequencies (0.5 Hz to 5 Hz) consistent with the frequency  
73 range of biomechanics applications, the footbridge vibration levels are well above the sensors'  
74 resolution levels and noise floors, and footbridge spans do not usually exceed the range limits for  
75 wireless transmission.

76 The typical civil field applications are time-constrained, logistically demanding and with restricted  
77 access for cabling. Hence a system that is readily transported, can be deployed rapidly and does not  
78 need cables is a very attractive proposition. The research described here aimed to find out if the  
79 limited resolution would be a show stopper for application in less lively structures such as tall  
80 buildings and road bridges.

81 This paper begins by describing how wired and wireless sensors are traditionally used for vibration  
82 testing, noting their strengths and limitations. A detailed comparison of performance IMUs with a

83 wired system is described for the floor mockup, followed by description of applications to a short  
84 span highway bridge and a nine-storey university building.

### 85 1.1. Wired accelerometer systems in modal testing of civil infrastructure

86 While only a single accelerometer is needed to estimate modal frequencies and damping ratios, full  
87 description of modal properties additionally requires estimation of mode shapes and modal masses,  
88 two properties frequently combined in the form of scaled mode shapes. Estimation of the full set of  
89 modal properties such as in ground vibration testing of aircraft [9] and vibration serviceability  
90 evaluation of lively floors in offices and hospitals [10] requires measurement of excitation force  
91 usually due to one or more shakers and acceleration response at multiple locations in a modal test  
92 [11]. Various techniques of experimental modal analysis (EMA) are applied to recover the modal  
93 properties and these require the force and response signals to be synchronised, since the  
94 identification processes rely on phase relationships between and among force and response signals.

95 Where a force signal cannot be provided or cannot be measured, output only or ambient vibration  
96 testing is used, and a range of techniques of operational modal analysis (OMA) are applied to  
97 recover all modal properties with the exception of modal mass or mode shape scaling. Typical  
98 applications of OMA include long span bridges [12], towers, chimneys [13] and tall buildings [14].  
99 The requirements of synchronous measurement of all response signals also apply.

100 Wired systems have varied architecture, with a large range of multichannel acquisition and analysis  
101 systems to choose from. The front end of such systems is nowadays typically a simultaneous sample  
102 and hold buffer to capture all signals at the same time instant, feeding a 24 bit analog digital  
103 converter which means that little or no signal amplification is required due to having bit-level  
104 precision below the sensor noise floor. With wired systems, choice of accelerometer and  
105 corresponding power supply signal conditioning allows for optimisation to application using high  
106 resolution sensors such as the PCB piezo-electric [15], Honeywell Quartz-Flex [16] or Kinemetrics  
107 servo- accelerometers [17]. An alternative to comprehensive signal analysis systems, bespoke  
108 systems built from multi-channel acquisition front ends in a component system (e.g. National  
109 Instruments) allow for flexible architecture providing signals for processing using separate modal  
110 analysis software.

### 111 1.2 Wireless sensing for civil engineering structures

112 The past two decades have seen significant effort on developing wireless sensing systems for civil  
113 engineering structures, especially bridges. This effort has been largely motivated by the logistical  
114 difficulties experienced when installing wired systems, however developments have been targeted  
115 at permanent monitoring systems rather than temporary systems. Hence wireless accelerometers  
116 developed and adapted by civil engineering researchers [18-20] have been optimised for low power  
117 operation with efficient real time data transmission and on board processing to reduce power  
118 requirements and the need for downstream data reduction. The ultimate wireless accelerometer  
119 demonstration is the Jindo Bridge project [21]. There are few applications of such wireless  
120 accelerometers for short term measurement campaigns such as modal testing [22,23] because their  
121 optimisation for long term monitoring and on-board processing means they are not well suited for  
122 the demands of a modal testing campaign.

123 While modal testing requires synchronous data acquisition, this does not necessarily mean that data  
124 must be transmitted to a base station for analysis in real time. Hence a system of autonomous  
125 recorders conventionally deployed in seismic monitoring, and with GPS synchronisation can be used  
126 for distributed data acquisition with data from separate units merged in post processing for modal  
127 analysis. Systems from Guralp and GeoSIG provide this capability and the latter was deployed for  
128 ambient vibration testing of Humber Bridge in 2008 [24]. In the absence of a GPS signal, precision  
129 clocks can be used to synchronise recorders [25-27] but these are usually for high-end applications,  
130 and there is justification for low-cost devices with limited capabilities and simple operation in certain  
131 circumstance. The aim of this paper is to show the capabilities and limitations of such a system.

### 132 1.3 Objectives

133 Wireless sensor systems for civil engineering structures have been optimised for long term  
134 monitoring and real time data transmission to a base station e.g. Imote2 [19]. For modal testing with  
135 tight timing and logistical constraints the time spent establishing a wireless network for real time  
136 transmission is not a good investment when reliable synchronous data collection is all that is  
137 needed. It is capability and performance in this respect that is investigated in this paper, as modal  
138 tests need to be time-efficient with easy to deploy accelerometers. Authors have found that a modal  
139 test (of a footbridge) can be reduced to carrying a handful of IMUs to site in a coat pocket, resting  
140 them on the bridge surface at selected measurement points for set duration then collecting the  
141 IMUs and returning to base. Subsequent downloading and merging of data from each IMU is equally  
142 simple. This paper explores the limits of capability of a particular type of IMU designed for  
143 biomechanics applications when used for modal testing of a representative set of civil structures.

144 Identifying capabilities and limitations will build confidence in using the IMUs for modal testing of  
145 specific structures by comparison with high resolution wired accelerometers, focusing on  
146 synchronisation and resolution. To begin, the IMUs and wired (reference) sensors are described in  
147 section 2, then the ability of the IMUs to capture the mode shapes is examined for three different  
148 structures: a laboratory floor structure (5 m x 7.5 m), a steel road bridge (36 m span), and a 7 story  
149 concrete office building. These results are reported in sections 3, 4 and 5 respectively. It is shown  
150 that broadly speaking the frequencies and mode shapes obtained from the IMUs agreed very well  
151 with those obtained from the wired system.

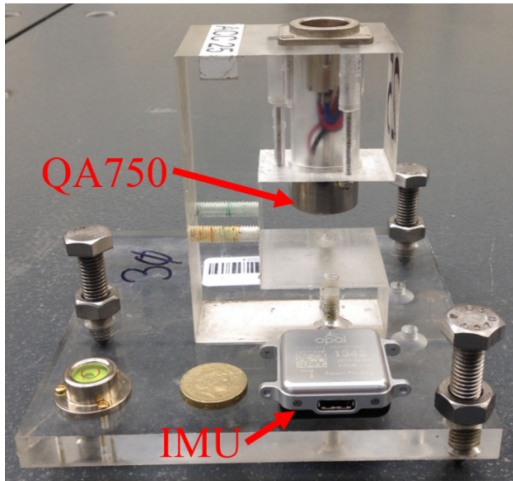
## 152 **2.0 Description of wired and wireless sensors used**

### 153 2.1 Wired accelerometers: Honeywell QA-750 force balance accelerometers

154 The reference accelerometers used here are Honeywell QA-750 quartz-flex force balance  
155 accelerometers. These are inertial grade uniaxial accelerometers historically used for inertial  
156 guidance (aerospace) and directional drilling (oil/gas industry). Their low noise floor and frequency  
157 response to DC has allowed their successful use for many years for the modal testing of a range of  
158 civil engineering structures. They are also used in the structural health monitoring systems installed  
159 on Hong Kong's long span bridges [28]. These accelerometers comprise a sprung proof mass moving  
160 in a magnetic coil whose current, generated by a servo-controller keeps the mass in position. For  
161 field testing described in this paper the current signal is dropped across an external 1 k $\Omega$  resistor so  
162 that effective scale factor is approximately 1.3 V/g and using a 24 bit analogue to digital converter  
163 (ADC) with  $\pm 5V$  range, bit level resolution is 0.155  $\mu g$  (1.52  $\mu m.s^{-2}$ ). The accelerometer is mounted in

164 a perspex housing shown in Fig. 1. This may be attached to a structure using glue or magnets, but  
165 more usually the housing is attached to a base plate with three levelling screws (Fig. 1) that rest on  
166 the horizontal surface of a structure whose vibration levels are usually a small fraction of gravity. The  
167 stiff mounting has no effect on the performance of the QA in the range of frequencies measured on  
168 civil structures.

169



170

171 Fig. 1, Honeywell QA 750 accelerometer mounted in perspex housing with Opal IMU left on the base  
172 plate.

## 173 2.2 Wireless accelerometers (IMUs)

174 The IMU used here is the APDM Opal™ shown in Fig. 1 placed on the perspex base plate of the QA-  
175 750 accelerometer. For size reference, a £1 sterling coin is also shown in the figure.

176 IMUs were originally developed for clinical research in biomechanics [29] and the fusion of data  
177 from three types of sensor promotes them to Attitude and Heading Reference Systems (AHRS). The  
178 Opal is one type of AHRS described in [29]. The on board magnetometer, triaxial accelerometer and  
179 triaxial gyroscope provide data on motion and orientation. Each Opal IMU also incorporates a  
180 temperature gauge, flash memory, and communication managed by an on-board microcontroller. In  
181 this study vertical and biaxial horizontal acceleration with respect to the local coordinate system of  
182 the IMU are used and the gyro and magnetometer data are not needed to transform accelerations  
183 to WCS. With the 14-bit ADC the  $\pm 2$  g and  $\pm 6$  g ranges offered correspond to bit-level resolution of  
184  $240 \mu\text{g}$  ( $2.35 \text{ mm.s}^{-2}$ ) and  $730 \mu\text{g}$  ( $7.19 \text{ mm.s}^{-2}$ ). For all the measurements described here the sample  
185 rate was set to 128 Hz per channel.

186 Of great importance to the performance of any compound (e.g. multi-agent/unit) wireless  
187 measurement system is the capability for synchronised data capture. Opal™ IMUs are synchronised  
188 in one of two ways, either with or without a wireless access point allowing rapid data streaming to  
189 the host computer. In the former mode, denoted as a synchronised streaming mode (SSM), any  
190 deviations in the timing of data collected by IMUs are adjusted to the master time of the host  
191 computer. Due to its dependence on access point connectivity, SSM is suitable for laboratory  
192 environments of relatively small dimensions. In the latter mode, denoted as synchronised logging

193 mode (SLM), the timing of data capture is adjusted according to a probabilistic model, based on a  
194 network of individual clocks of all units. The data are recorded onto the memory of each unit and  
195 downloaded offline via a docking station. SLM is suitable for applications in which immediate data  
196 accessibility is not of critical importance.

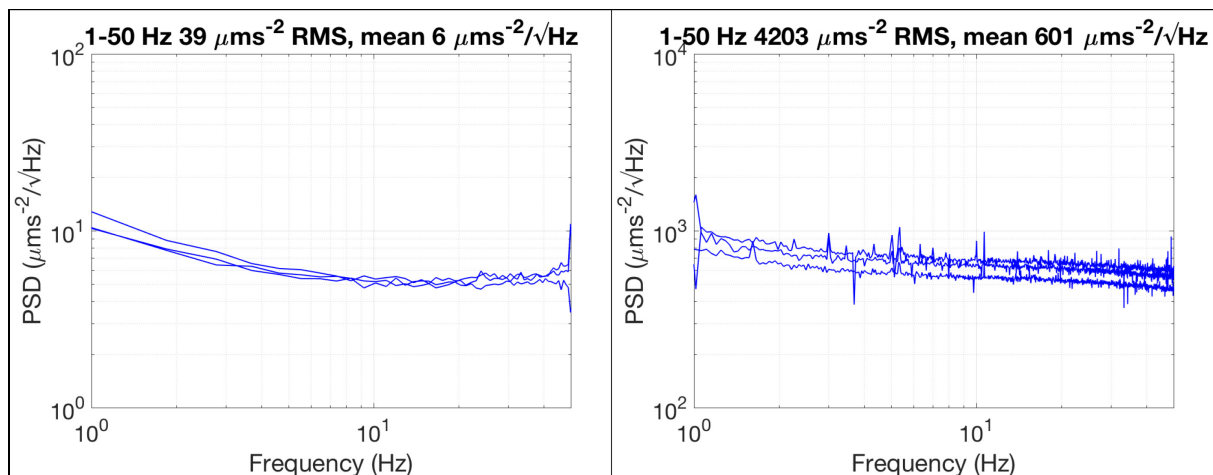
197 When operating in SSM the IMUs need to remain within 30 m of the wireless access point to  
198 maintain synchronisation. Definite information on the maximum distance between IMUs allowing  
199 synchronisation to be maintained when operating in SLM is not available. Essentially, having been  
200 developed for applications in biomechanical research, situations where the IMU were tens of meters  
201 apart were unlikely to occur. In this study the sensors will be used in SLM as the requirement to set  
202 up a wireless access point on a civil engineering structure is logistically undesirable. In SLM if the  
203 IMU's are out of range with each other they each keep time using their own internal clock. Once this  
204 occurs, some drift is possible between individual sensors, with larger drifts likely if there are large  
205 temperature ranges among sensors. Synchronisation drift is an important issue as it can affect modal  
206 analysis procedures [30], but because wireless communication and synchronisation effects on modal  
207 analysis are affected by a very wide range of factors it is not studied here. Instead the aim is to  
208 examine if the potential errors identified above are sufficiently small that the mode shapes obtained  
209 based on data from IMUs are still identified correctly.

210 As part of a previous study [31] it was shown that IMU's could be used to capture the mode shapes  
211 of a relatively flexible cable supported footbridge. However, significant questions remained as to  
212 how the IMUs would perform on more common civil engineering structures such as road bridges and  
213 office towers, where the amplitudes of vibration will be significantly smaller than on a cable  
214 supported footbridge and synchronisation between sensors could be affected by larger distances  
215 and physical barriers such as walls/floors between the IMUs. These questions are addressed in this  
216 current work.

### 217 2.3 Sensor noise floor

218 Manufacturer data for the two sensors quotes sensor noise floor for the QA-750 as  $7 \mu\text{g}/\sqrt{\text{Hz}}$  in 0-10  
219 Hz band and for the Opal™ as  $128 \mu\text{g}/\sqrt{\text{Hz}}$ . A test of the sensors in quiet laboratory conditions was  
220 used to check these figures. In two separate exercises in different laboratories and times, signals  
221 from three co-located sensors were acquired. Any coherent response due to small vibrations in the  
222 quiet laboratory is filtered to leave non-coherent signals representing noise [32]. The result is shown  
223 in Fig. 2. In both cases the self-noise is below the manufacturer specification and in fact the Opal  
224 self-noise, for the sensor operating in the 6 g range, is below the bit-level resolution. The Opal noise  
225 floor is 10 times greater than for the QA.

226 The effect of sensor noise floor on accuracy of modal identification is beyond the scope of this paper  
227 although recent research [33] has been able to quantify the effect of (response) signal to (sensor)  
228 noise ratio for Bayesian operational modal analysis. A pilot study [26] comparing IMUs and QA for  
229 ambient response of a footbridge has shown that the effect of IMU noise floor on frequency and  
230 damping estimation uncertainty in one specific application is insignificant.



231 Fig. 2, Power spectral density of sensor self-noise for QA-750 (left) and Opal IMU (right).

### 232 3.0 Laboratory Trial

233 The laboratory trial was split into two parts. Initially both sensors (QA and IMU) were placed on a  
 234 shaker to see how the IMU performed relative to the QA across a range of amplitudes and  
 235 frequencies (section 3.1). Subsequently data from both sensors were used to calculate the mode  
 236 shapes of a steel floor structure that was built in the laboratory (section 3.2). Essentially Section 3.1  
 237 checks the sensitivity/performance of the accelerometer in the IMU across the range of acceleration  
 238 amplitudes and structural frequencies typically encountered on civil engineering structures and  
 239 section 3.2 checks if under laboratory conditions the synchronisation between the different IMUs in  
 240 the network is sufficiently accurate to allow mode shapes to be recovered accurately.

#### 241 3.1 Performance of accelerometers when placed on shaker

242 Authors' experience of using the QA is that it is both accurate and reliable and hence very well suited  
 243 to the demands modal testing of civil structures, but there are occasions when the full capability is  
 244 not required and the expense not justified. Also technology developments lead to lower cost MEMS  
 245 sensors that approach or even exceed the performance of QAs, which are regarded by authors as  
 246 the standard against which all other accelerometers are judged.

247 Accelerometer calibration is provided by the manufacturers. For the QAs the calibration certificates  
 248 state current output in mA/g which is converted to V/g using precision 1 kΩ load resistors, while for  
 249 the IMUs the signals are converted to m.s<sup>-2</sup> by on board processor. In each case a simple check is  
 250 obtained using the 1 g signal offset when measuring vertical acceleration. Using this methods, the  
 251 set of five IMUs used in the experiment to generate Fig. 2 report gravity as 9.864 m.s<sup>-2</sup> with standard  
 252 error 0.6% while the set of four QAs report gravity as 9.8305 with standard error 0.3%.

253 To examine how well the IMU performed with respect to the QA both sensors were mounted on a  
 254 shaker (see Fig. 3) and a white noise excitation signal was provided to the shaker. The IMU was  
 255 operating in SLM. The test lasted for approximately 10 minutes (600 seconds) and the time series  
 256 recorded by both accelerometers (scanning rate 128 Hz) is shown in Fig. 4(a). The shaker was driven  
 257 at a quarter of maximum force output to generate maximum accelerations in the region of ±1 m/s<sup>2</sup>  
 258 which is the typical range of accelerations encountered on civil engineering structures. Fig. 4(b)  
 259 shows a zoomed in view of one second of acceleration data and it can be seen that there is good

260 agreement between the signals from both accelerometers. The Welch method was used to calculate  
 261 the frequency content of both signals in Fig. 4(a), with window length of 60 seconds, with no  
 262 overlap, and the result is shown in Fig. 4(c). It can be seen in Fig. 4(c) and Fig. 4(d), which shows a  
 263 zoomed in view between 4-5 Hz that the frequency content returned by both sensors is very similar.  
 264 To further examine how closely the signal from the IMU matches the signal from the QA, the  
 265 transfer function ( $T_{qo}(f)$ , Eq. 1) and magnitude squared coherence ( $C_{qo}(f)$ , Eq. 2) between the QA and  
 266 the IMU are calculated and the results are plotted in Figs. 4(e) and (f) respectively.

$$267 \quad T_{QI}(f) = \frac{P_{IQ}(f)}{P_{QQ}(f)} \quad (1)$$

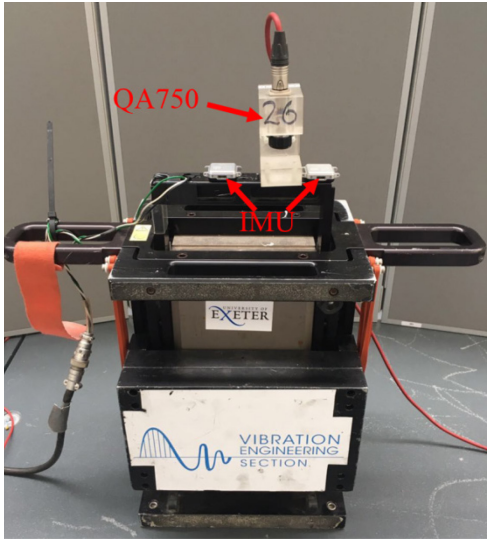
268

$$269 \quad C_{QI}(f) = \frac{|P_{IQ}(f)|}{P_{QQ}(f) P_{II}(f)} \quad (2)$$

270

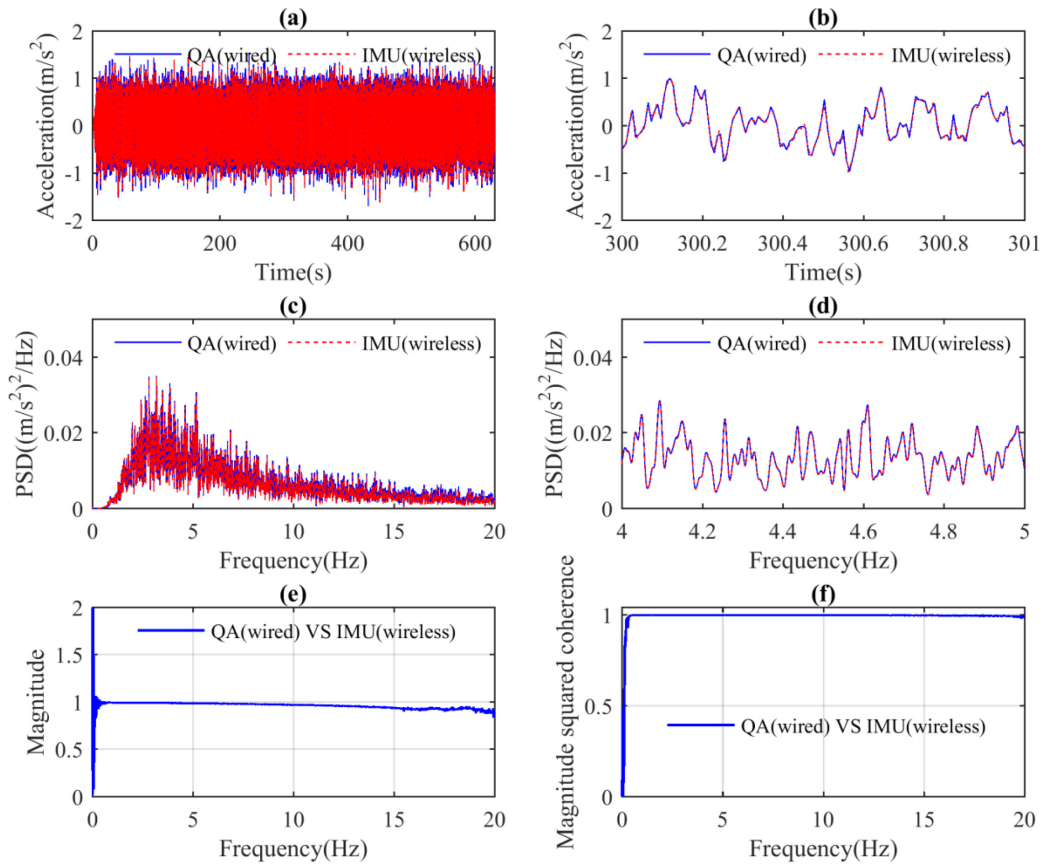
271 where  $P_{IQ}$  is the spectral density of the QA signal and the IMU signal,  $P_{QQ}$  is the power spectral  
 272 density of the QA signal, and  $P_{II}$  is the power spectral density of the IMU signal. For both metrics  
 273 ( $T_{QI}(f)$  &  $C_{QI}(f)$ ) values of close to one indicates a good match between the signals being analysed.  
 274 Broadly speaking the plots in Figs. 4(e) and (f) remain close to one in the frequency range 0-20 Hz,  
 275 with just the transfer function falling slightly below one for higher values of frequency. This indicates  
 276 that for frequencies in the range 10-20 Hz the IMUs may be slightly less accurate than the QAs  
 277 however, overall the IMU compares very well with the QA. To examine if the amplitude of the  
 278 acceleration signal affected the performance of the IMU (with respect to the QA) similar tests were  
 279 performed at 50% and 75% of full shaker force output, leading to acceleration signals with  
 280 amplitudes of  $\pm 2 \text{ m/s}^2$  and  $\pm 3 \text{ m/s}^2$  respectively. Plots almost identical to those shown in Fig. 4 were  
 281 obtained, with the only difference being that the transfer functions for higher amplitude  
 282 acceleration signals decline more gently than shown in Fig. 4(e). Essentially for larger amplitudes of  
 283 acceleration the IMUs provide a performance even closer to the performance of the QA. This is to be  
 284 expected, the higher sensor noise of the IMU (see section 2) becomes less of an issue for higher  
 285 values of acceleration.

286 For the vast majority of floors and footbridges vibration serviceability is not a problem. However, for  
 287 a small subset of these structures users report vibration serviceability issues, and modal tests are  
 288 often commissioned by the structure owner. The experience of the authors in doing these kinds of  
 289 modal tests is that signal levels of  $\sim \pm 1 \text{ m/s}^2$  and frequencies of 0-20 Hz are fairly typical of these  
 290 'lively' footbridges and floors and in these applications the accelerometer in the IMU works well.  
 291 However, capabilities at lower signal levels and to identify mode shapes remain to be tested, and  
 292 these will be examined in subsequent sections. In particular IMUs must also remain accurately  
 293 synchronised for the duration of the test so that modal analysis algorithms can work [30]. The ability  
 294 of the IMU network to remain synchronised in laboratory conditions is examined in the next section  
 295 where IMUs are used to determine the mode shapes of a laboratory floor structure having relatively  
 296 high natural frequencies.



297

298 Fig. 3, IMU and QA on shaker.



299

300 Fig. 4, results from shaker test (a) full time history (b) zoomed in view on a portion of the time series,  
 301 (c) frequency content of time series shown in (a), (d) zoomed in view of frequency content, (e)  
 302 Transfer function between QA and IMU, (f) Magnitude squared coherence between QA and IMU.

303

304 3.2 Modal test of floor structure

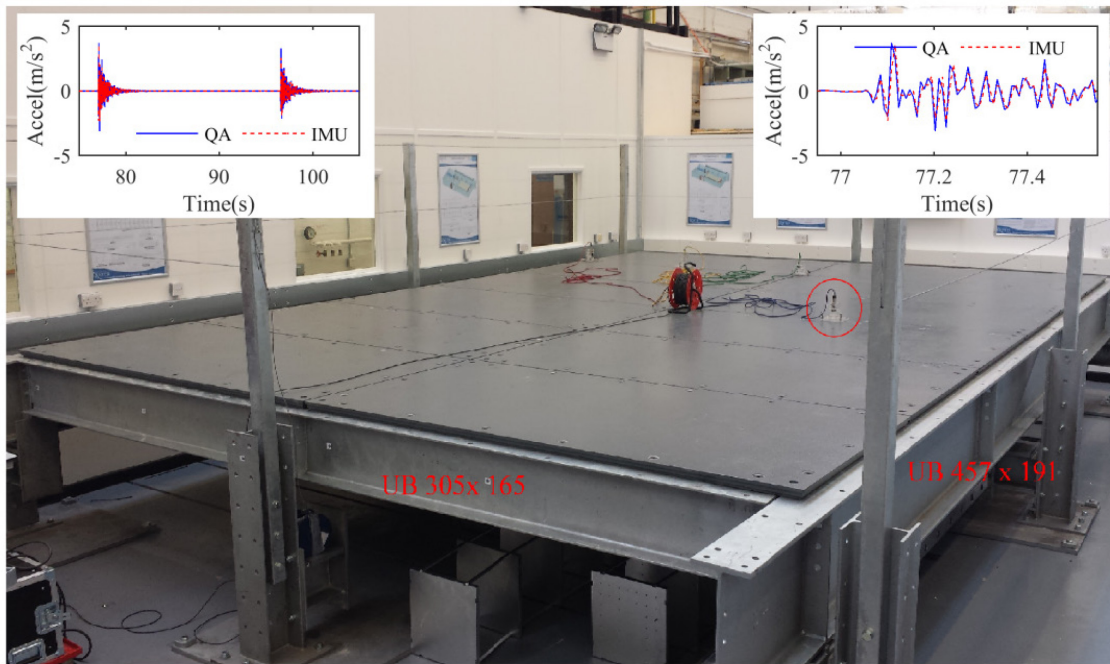
305 **3.2.1 Experimental setup for modal test on lab structure**

306 The test structure is the 5m x 7.5m steel floor structure shown in Fig. 5, the structure is supported  
307 only at the corners. The structure consists of a series of steel plates supported on steel beams. The  
308 two longitudinal beams (UB 475x191) span 7.5m between the supports. The transverse beams (UB  
309 305x165) are 5.0m long and they span between the longitudinal beams, these beams are indicated  
310 in Fig. 5. Finally an internal longitudinal beam (UC 203x203) spans between the two end transverse  
311 beams. This beam is under the slab and therefore is not visible in the figure. The slab is formed using  
312 42mm thick plates, and these span between the longitudinal beams. The plates are Sandwich Plate  
313 System (SPS) plates manufactured by Intelligent Engineering and consist of two metal plates bonded  
314 with a polyurethane elastomer core.

315 In total 35 test points were used in the modal survey, the test grid having 5 test points in the  
316 transverse location and 7 in the longitudinal direction. The position of the sensors' locations can be  
317 understood by examining the grid shown in Table 1. On the day of the test only 4 QA accelerometers  
318 were available so one accelerometer was left at TP 25 as a reference (circled in Fig. 5) and it  
319 remained in this location for the duration of the test. During the test one IMU was 'paired' with each  
320 one of the four QA's by simply leaving it on the base plate of the QA as shown in Fig.1, and all of the  
321 IMUs were operating in SLM. Then over the course of 12 swipes the 3 (roving) accelerometers roved  
322 to the remaining 34 points. For example the photo in Fig. 5 shows the position of the accelerometers  
323 for swipe 6 where the reference accelerometer is at test point 25 and the three roving  
324 accelerometers are at test points 6, 13 and 20 respectively. For each swipe the structure was excited  
325 by a person doing a series of heel drops, typically six heel drops were carried out and each swipe  
326 took approximately 4 minutes to record. To excite as many modes as possible the person was  
327 standing at the centre longitudinally but slightly off centre transversely. The scanning frequency for  
328 both the QA and IMU sensors was 128 Hz. The acceleration recorded at test point 25 due to two  
329 consecutive heel drops close to the centre of the floor structure is shown as an insert in the top left  
330 of Fig. 5. A zoomed in view of the first heel strike is shown in the insert in the top right of the figure  
331 and it can be seen that there is good agreement between the two signals.

332 Finally it should be noted that in a laboratory environment, while it is quicker to collect the data with  
333 the IMUs than with the QA's the difference is not so pronounced. This is because in the laboratory  
334 there is ready availability of power, there is no need to shelter the logging station, and we are free to  
335 run cables wherever we want. However, in the next section it is shown that when collecting data on  
336 a road bridge the IMU's prove vastly quicker/easier to use than the QA's.

337



338

339 Fig. 5, Test floor structure in the laboratory and accelerometer locations for swipe 6 of the modal  
 340 test.

341

### 342 3.2.2 Modal identification procedure

343 After the lab testing a sequence of twelve four-minute recordings were available for the QA data.  
 344 After the lab test the four IMU's were placed in the docking station and the data from the entire test  
 345 were downloaded. Subsequently these data were split time-wise into twelve four-minute recordings  
 346 corresponding to the twelve QA recordings. The modal analysis procedure used to identify the mode  
 347 shapes in the QA and IMU data was exactly the same.

348 The method used is the NExT/ERA operational modal analysis procedure [34]. This is one of several  
 349 possible operational modal analysis procedures [35-37] and was used here due to long experience in  
 350 its use and implementation in bespoke software [38]. NExT/ERA is now a standard procedure so  
 351 only a very brief overview of the procedure as applied to these data is provided below.

352 Eigensystem Realization Algorithm (ERA) was put forward in the 1980's by Juang and Pappa [39] for  
 353 modal identification. In their original work Juang and Pappa applied ERA to free vibration response  
 354 following random excitation of the structure using electro-dynamic shakers. By the mid 1990's there  
 355 was a growing acceptance that conventional modal analysis techniques which required forced  
 356 excitation were inappropriate for a number of structures, particularly civil engineering structures.  
 357 Consequently James et. al. [40] proposed the Natural Excitation Technique (NExT) that allowed  
 358 structures to be tested in their ambient environments. The NExT method works by calculating auto-  
 359 and cross-correlation functions of the ambient time histories. Subsequently these correlation  
 360 functions are treated as if they were free vibration responses, to which it is possible to apply time  
 361 domain identification schemes such as ERA. In later years, when using the NExT methodology many  
 362 authors used ERA as the time domain identification scheme and consequently when discussing the  
 363 NExT methodology it is often referred to as NExT/ERA. While NExT/ERA is usually applied to ambient

364 vibraton due to borad band random or near-random excitation (e.g. wind, road traffic), due to the  
365 origion of the technique it also works well with induced transient response. In fact the transient  
366 acceleration response to a heel drop resembles the auto/cross correlation time series generated by  
367 NExT.

368 Each of the twelve recordings was truncated to 200 seconds as five consecutive 40-second frames.  
369 For each swipe a 4x4 cross-spectral density (CSD) matrix was created using the Welch procedure  
370 [41] without overlap or windowing, resulting in twelve CSD matrices corresponding to the twelve  
371 swipes. Subsequently each of these CSD matrices were normalised with respect to the reference  
372 sensor by dividing each frequency line/layer of the CSD matrix by the auto-power of the reference  
373 sensor. This normalisation allows the twelve individual CSD matrices to be merged into a single  
374 35x35 'global' CSD matrix.

375 Using an inverse Fourier transform the global CSD matrix was transformed to time domain as  
376 impulse response functions (IRFs) for the ERA procedure for recovery of the modal properties. Based  
377 on this, a set of five modes is visible up to 32 Hz. For both the QA and IMU data the NExT/ERA  
378 procedure produced a clean set of modes, which are presented in the next section.

### 379 **3.2.3 Results of test on lab structure**

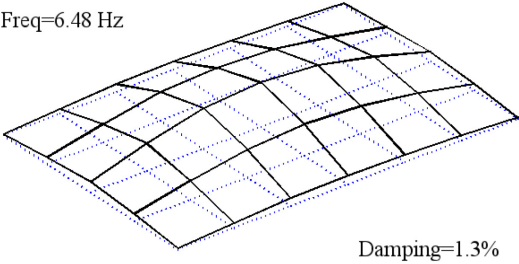
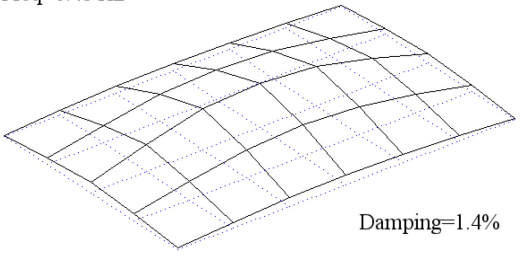
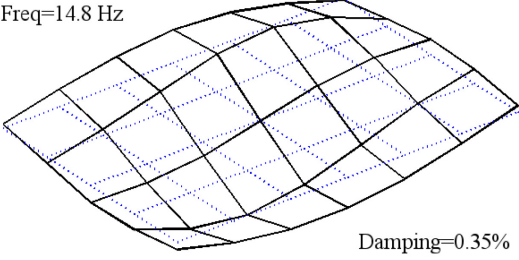
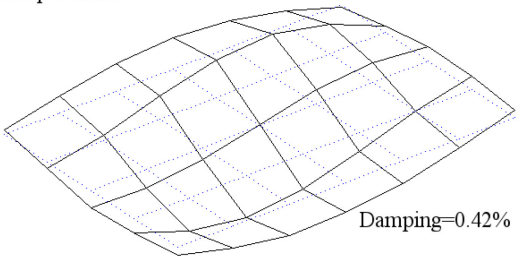
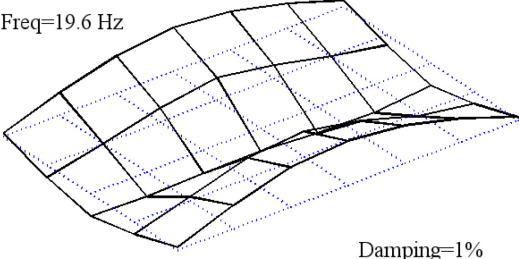
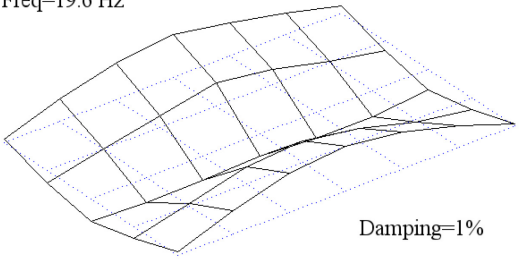
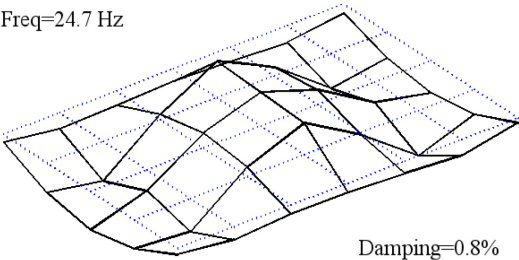
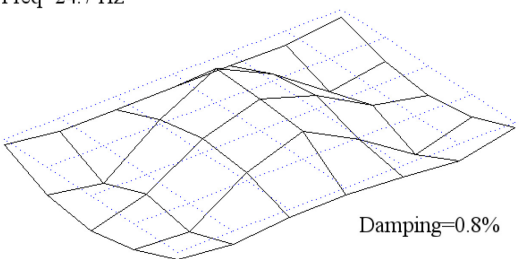
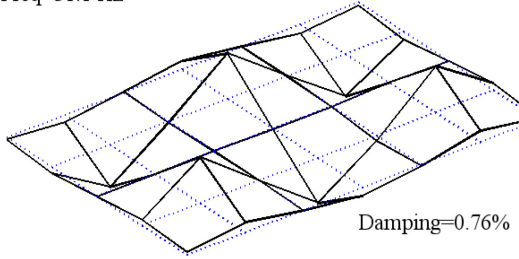
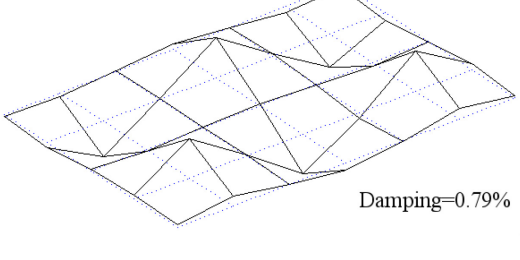
380 Using the modal analysis approach described in section 3.2.2 the mode shapes and frequencies  
381 shown in Table 1 were obtained. It can be seen that mode shapes calculated from the IMU data  
382 agree very well with those calculated from the QA data. This indicates that the IMUs remained  
383 synchronised for the duration of this test. In addition, the level of damping calculated is a very good  
384 match between the QA and IMU sensors. This demonstrates that under laboratory conditions,  
385 where the IMUs remain relatively close together, data collected from them can be used to  
386 determine the mode shapes of the structure.

387 Rather than relying on a single numerical indicator such as modal assurance Criteria (MAC), we  
388 prefer visual inspection of the mode shapes which can reveal differences that MAC obscures.  
389 Inspection of Table 1 shows that all features of the mode shapes are identified equally well using the  
390 IMUs.

391 In a laboratory setting where IMUs maintain continuous wireless communication between each  
392 other gross synchronisation errors would be prevented so a short measurement is enough to check  
393 for minor errors of timing between the IMUs. These would have a proportional greater effect at  
394 higher frequencies so the good comparison of the highest frequency modes suggests that there is  
395 neither monotonic drift nor small timing variation of any consequence for modal identification when  
396 used for testing structures of this scale. However, before further conclusions can be drawn on the  
397 applicability of the IMU's for the modal testing of structures it is necessary to test them on real  
398 structures in the field. Conditions in the field may be more challenging, e.g. levels of vibration may  
399 be smaller and/or the conditions may be such that the sensors lose wireless contact and as a result  
400 may lose synchronisation. Therefore field tests on a steel road bridge and a seven story office tower  
401 were carried out and are reported in sections 4 and 5 respectively.

402

403 Table 1, Frequencies, damping coefficients and mode shapes for the first 5 vertical modes

Mode No	QA	IMU	% Freq Diff*
1	<p>Freq=6.48 Hz</p>  <p>Damping=1.3%</p>	<p>Freq=6.48 Hz</p>  <p>Damping=1.4%</p>	0%
2	<p>Freq=14.8 Hz</p>  <p>Damping=0.35%</p>	<p>Freq=14.8 Hz</p>  <p>Damping=0.42%</p>	0%
3	<p>Freq=19.6 Hz</p>  <p>Damping=1%</p>	<p>Freq=19.6 Hz</p>  <p>Damping=1%</p>	0%
4	<p>Freq=24.7 Hz</p>  <p>Damping=0.8%</p>	<p>Freq=24.7 Hz</p>  <p>Damping=0.8%</p>	0%
5	<p>Freq=31.1 Hz</p>  <p>Damping=0.76%</p>	<p>Freq=31.1 Hz</p>  <p>Damping=0.79%</p>	0%

\* Percentage difference between the IMU frequency and QA frequency

## 404 4.0 Field test on steel road bridge

### 405 4.1 Description of bridge

406 Fig. 6 shows the bridge used in this experiment and a plan view of the bridge is shown Fig. 7. The  
407 bridge is a half through steel girder bridge, it spans 36 m and the deck is simply supported. The 7.6 m  
408 wide, 200mm deep, concrete deck is supported on a series of 450 mm deep steel beams spanning  
409 transversely between the main girders which are approximately 2 m deep.

410  
411



412  
413 Fig. 6, Bridge used in field test.

### 414 4.2 Collecting acceleration data

415 This section describes installing a conventional sensing system on a live bridge (section 4.2.1), and  
416 the procedure for installing wireless IMUs (section 4.2.2).

417 Using wired accelerometers in the field requires a logging station to be set up and wires installed to  
418 connect each sensor to the logging station. Conventional wireless systems described in section 1 still  
419 require a logging station but the sensors are connected wirelessly to the logging station for wireless  
420 streaming of the data. However, it is not uncommon to have to spend time finding the necessary  
421 uninterrupted lines of sight for the wireless system to work properly.

422 So in both a wired arrangement and a conventional wireless system there is (i) a logging station and  
423 (ii) a system to transmit data from the sensor to the logging station. The IMUs require neither (i) nor  
424 (ii) because the data is logged at source and synchronisation is implemented by the sensors  
425 communicating with each other to ensure time synchronisation. Not having to install (i) and (ii)  
426 makes collecting field data with the IMUs vastly easier. The wired test described in section 4.2.1 took  
427 one person several days to plan and four people one day to execute. Planning and executing the test  
428 with the IMU system (section 4.2.2) took one person approximately 1 day.

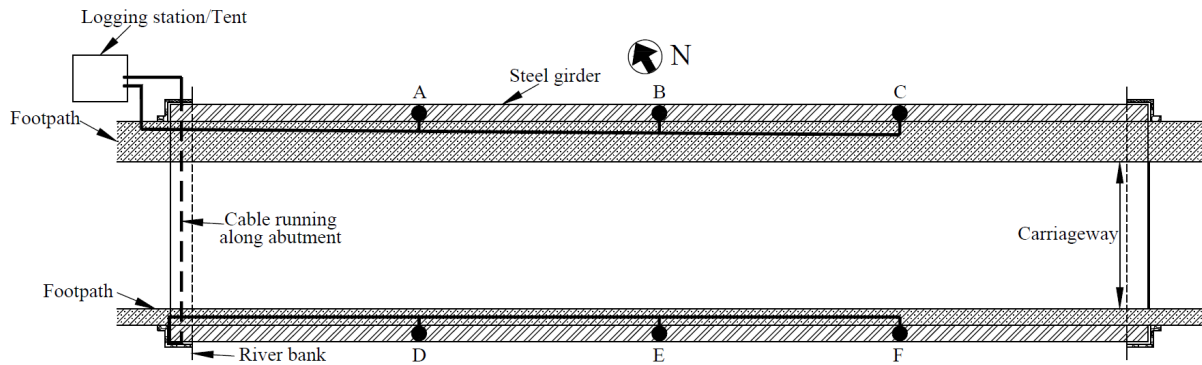
429

#### 430 4.2.1 Wired system (QAs)

431 Fig. 7 shows a plan view of the bridge and the accelerometer locations used. Accelerometer  
432 locations A, B & C were at the  $\frac{1}{4}$  point, mid-span and  $\frac{3}{4}$  point of the deck on the north side of the  
433 bridge, locations D-F were at the same longitudinal positions on the south side of the deck. The data  
434 logging tent was set up at the northwest corner of the bridge and this is indicated in the top left of  
435 the figure. The accelerometer at location B is shown in Fig. 8(c), the accelerometer is attached to the  
436 underside of the top flange via a magnet, and the signal is carried to the data logger via the cables

437 visible in the image. A schematic of the route taken by the cables is indicated in Fig. 7. Carrying the  
438 signal from the sensors on the south side of the bridge to the logger was logistically difficult as it is  
439 necessary to run a cable under the bridge deck (along the abutment shelf) which is slow and risky to  
440 install when the bridge spans over a river. A view of the logging tent is shown in Fig. 8(a) and the  
441 logging equipment used is shown in Fig. 8(b). In total acceleration was recorded for approximately  
442 45 minutes and Fig. 8(d) shows the typical acceleration response recorded at sensor location B as a  
443 car crossed over the bridge.

444  
445



446  
447 Fig. 7, schematic of the accelerometer locations A-F and corresponding cabling arrangement.

448  
449 Carrying out the test described above takes a significant amount of time with most of the time being  
450 spent in the planning phase. The planning phase takes time because (1) installing cabling on a live  
451 bridge and erecting a logging station in a public area requires various health and safety permissions  
452 be applied for, and (2) the amount of equipment required to be brought to site (sensors, cabling,  
453 logging equipment, power source etc.) takes time to organise. But even once on site, setting up and  
454 demounting the equipment takes 3-4 people several hours.

455  
456  
457  
458  
459  
460  
461  
462  
463



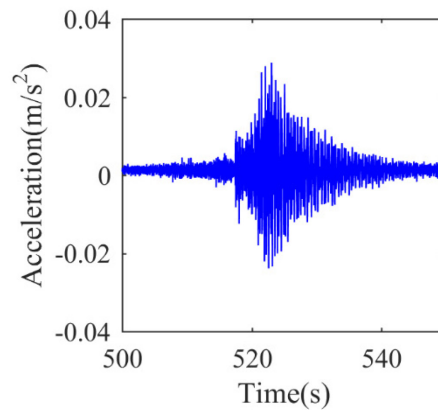
(a)



(b)



(c)



(d)

464  
 465 Fig. 8, Test set up for wired test (a) tent for data logging equipment positioned at northwest corner  
 466 of bridge (b) logging equipment inside the tent, (c) accelerometer attached to underside of girder  
 467 flange and associated cabling, (d) bridge acceleration response to a passing car

468

#### 469 4.2.2 Wireless system (IMUs)

470 When collecting the data with the IMUs the same accelerometer locations (A-F in Fig. 7) were used.  
 471 Fig. 9 shows the girder on the south side of the bridge and it can be seen that there is a horizontal  
 472 steel member running along the length of the girder. The IMUs were attached to the bridge by  
 473 taping them to this member, and a zoomed in view is shown in the insert of the figure. Mounting the  
 474 IMUs adjacent to the vertical web stiffeners ensures the sensor is only picking up global bridge  
 475 vibrations rather than local vibrations of the horizontal member. IMUs mounted at locations F, E & D  
 476 are indicated in the figure. Acceleration was recorded for 45 minutes and acceleration response  
 477 recorded by the IMU at mid-span due to the passage of a car looked very similar to the signal shown  
 478 in Fig. 8(d). As collecting the data with the IMU's essentially requires just 6 sensors to be mounted  
 479 locally on the bridge the health and safety permissions are minimal, and therefore very  
 480 quickly/easily obtained. The planning phase is practically non-existent as the only equipment  
 481 required to be brought to site are six IMUs that can be carried in a coat pocket. Once on site one  
 482 person can install and (once the test is complete) demount the sensors in approximately 10 and 5  
 483 minutes respectively. So relative to the man hours required to collect the data with a wired system  
 484 collecting the data with the IMUs takes vastly less time. The mode shapes identified by both systems  
 485 are presented in the next section.



486

487 Fig. 9, IMUs deployed at sensor locations F, E & D (see Fig. 7), insert shows how IMUs were simply  
488 taped to the horizontal member adjacent to the vertical web stiffener.

#### 489 4.3 Mode shapes from road bridge

490 The modal identification procedure described in section 3.2.2 was implemented to identify the mode  
491 shapes from both the QA and IMU data and the results are shown in Table 2. Similar to the floor  
492 structure the mode shapes and frequencies calculated using the IMU sensors compares very well  
493 with those calculated using the wired QA system. There are some differences in the frequencies  
494 observed but it should be noted that the data for both systems were collected on different days and  
495 the day of the IMU test was colder, so some small differences in frequencies are to be expected [42].  
496 The results shown in table 2 demonstrate primarily two things, firstly when the amplitude of  
497 acceleration is in the region of  $\pm 0.1 \text{ m/s}^2$  or greater the IMUs will be able to capture the vibration.  
498 Secondly when contained in an open area (18 m x 9 m) the IMUs remain sufficiently well  
499 synchronised to capture the mode shapes. This is believed to be because the distance between  
500 individual IMUs is sufficiently small that mesh synchronisation algorithm remains working. To further  
501 explore the capabilities of the IMUs for modal testing in the next section more challenging test  
502 environment is examined in the form of a 7 storey office tower. In the tower the vibrations are less  
503 than  $0.1 \text{ m/s}^2$  and the IMUs will be separated by walls and concrete floors.

504

505

506

507

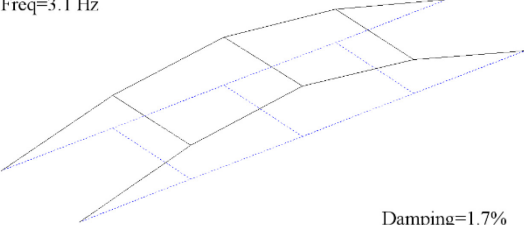
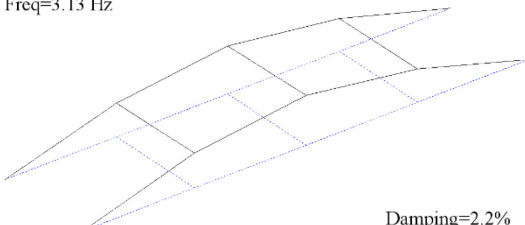
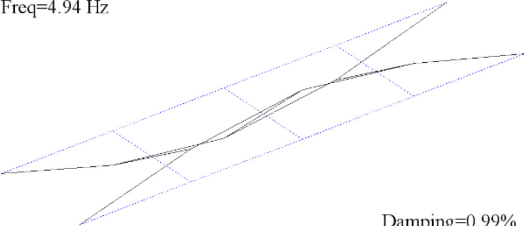
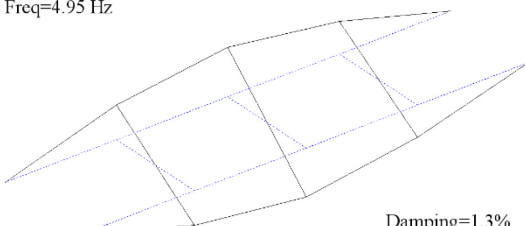
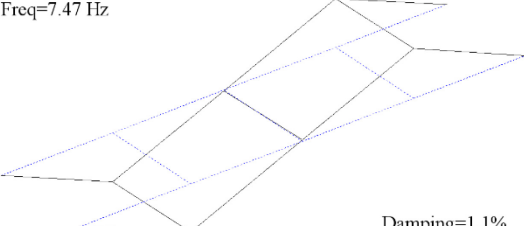
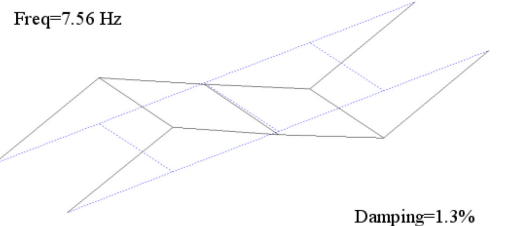
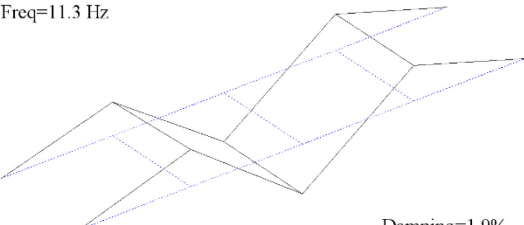
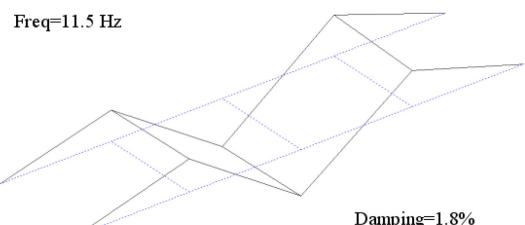
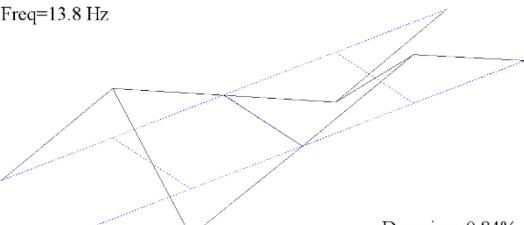
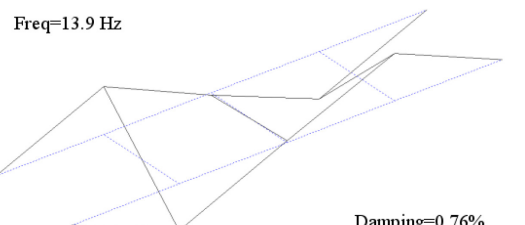
508

509

510

511

512 Table 2, Frequencies and mode shapes for the first 5 vertical modes

Mode No	QA	IMU	% Freq Diff*
1	<p>Freq=3.1 Hz</p>  <p>Damping=1.7%</p>	<p>Freq=3.13 Hz</p>  <p>Damping=2.2%</p>	0.95%
2	<p>Freq=4.94 Hz</p>  <p>Damping=0.99%</p>	<p>Freq=4.95 Hz</p>  <p>Damping=1.3%</p>	0.20%
3	<p>Freq=7.47 Hz</p>  <p>Damping=1.1%</p>	<p>Freq=7.56 Hz</p>  <p>Damping=1.3%</p>	1.20%
4	<p>Freq=11.3 Hz</p>  <p>Damping=1.9%</p>	<p>Freq=11.5 Hz</p>  <p>Damping=1.8%</p>	1.77%
5	<p>Freq=13.8 Hz</p>  <p>Damping=0.84%</p>	<p>Freq=13.9 Hz</p>  <p>Damping=0.76%</p>	0.72%
* Percentage difference between the IMU frequency and QA frequency			

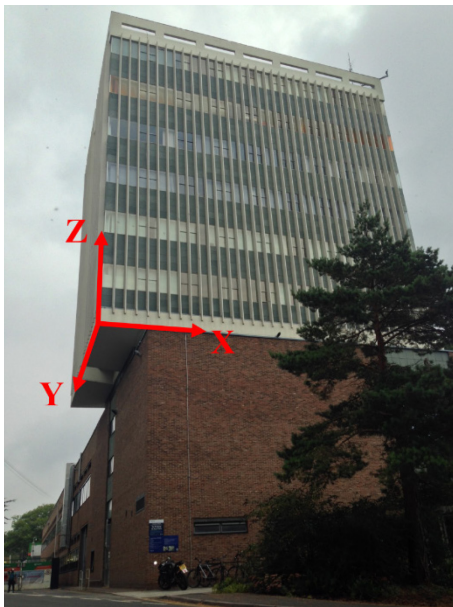
513

514

515 **5.0 Field test on 7 storey concrete office tower**

516 5.1 Description of tower

517 The building used in the test is shown in Fig. 10. Structurally the tower is a little unusual in that  
518 floors 2-7 have slightly larger plan dimensions than the lower floors. This can be seen in Fig. 10  
519 where the second floor overhangs the lower floors. The plan dimensions of floors 2-7 is 22m x 16m  
520 in the x and y directions respectively. For ease of visualisation horizontal x and y axes are indicated in  
521 the figure. In Fig. 10 it can be seen that the ground floor and first floor of the building are much  
522 longer in the y-direction. For the purposes of this test only tower vibrations are recorded, i.e. no  
523 data is recorded in other parts of the building. In total the tower has 10 floors, namely; basement,  
524 ground floor, first floor, mezzanine floor, second floor, and floors 3-7. For visualisation purposes a  
525 3D schematic of the building is shown in Fig. 12, however for simplicity, the overhang at the 2<sup>nd</sup> floor  
526 is not indicated. Lateral stability for the tower is provided by a reinforced concrete stairwell and lift  
527 core. A schematic of the floor plan for floors 7, 5 and 3 are shown in Figs. 11(a-c) respectively.



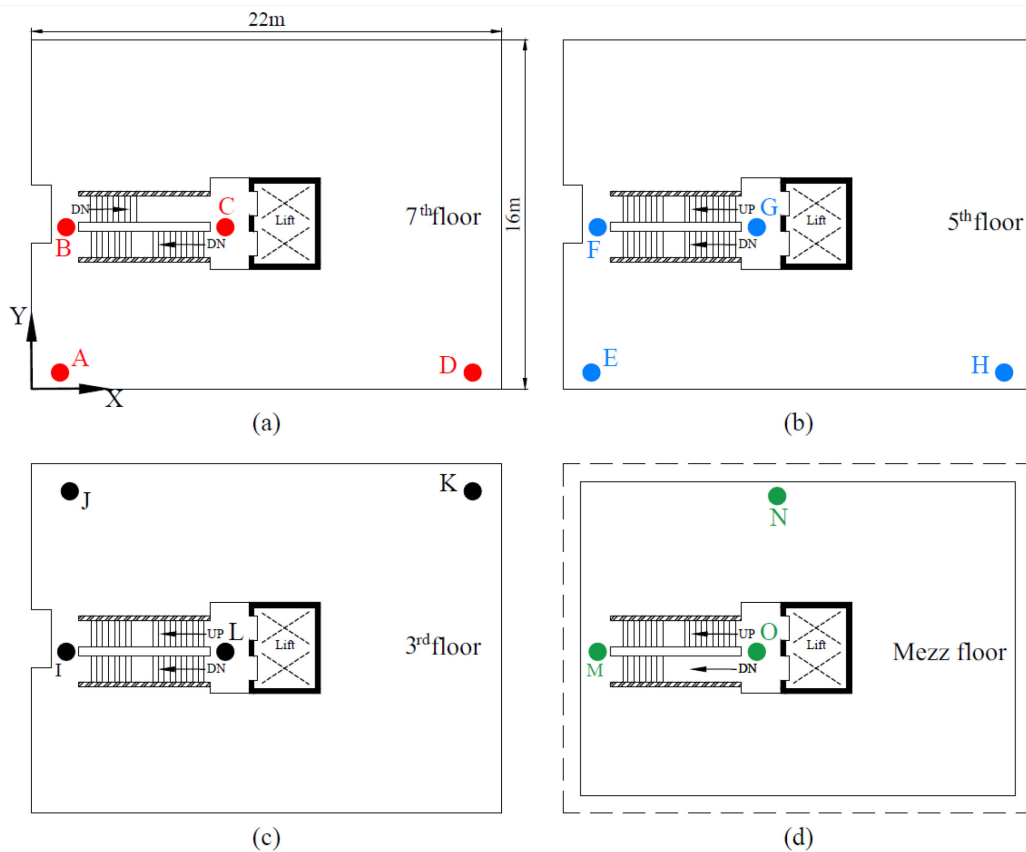
528  
529 Fig. 10, Tower used in test.

530

531 5.2 Collecting acceleration data

532 In this test acceleration is recorded four separate floors, namely floors 7, 5, 3 and the mezzanine  
533 floor and the location of the test points used on each floor are indicated in Fig. 11 using circular dots.  
534 The schematic in Fig. 11 does not show the room layout in the building (i.e. non-structural walls have  
535 been omitted) and as a result the irregular test points (on each floor) initially look a little odd.  
536 However, on the night of the test the monitoring team did not have access to all parts of the building  
537 and therefore accelerometers had to be located where access was permitted. In total acceleration  
538 was recorded at fifteen different test points in the building labelled A-O in Fig. 11, four test points on  
539 each of floors 7, 5, and 3, and three test points on the mezzanine floor.

540



542

543 Fig. 11, schematic floor plans of the tower and test points used in modal test (a) 7<sup>th</sup> floor, (b) 5<sup>th</sup>  
 544 floor, (c) 3<sup>rd</sup> floor, (d) mezzanine floor.

545 Each test point required two QA accelerometers to measure acceleration in the x and y directions,  
 546 and one IMU, (the IMU has a triaxial accelerometer so only one IMU is required per test point). Both  
 547 the QAs and the IMUs were scanning at 128 Hz and the typical accelerometer arrangement at a test  
 548 point is shown in Fig. 13(a). Due to the limited number of sensors available the data were collected  
 549 in a number of 'swipes'. Table 3 gives a summary of the test points where acceleration was being  
 550 recorded during a given swipe. It can be seen in the right hand column of Table 3 that test point A is  
 551 included in all four swipes, this is to allow the data from the different swipes to be 'glued' together  
 552 in post processing. To allow a 3D visualisation of where test points A-O are located in the building  
 553 the approximate positions of the test points on each floor are shown in Fig. 12. Test point A on the  
 554 7<sup>th</sup> floor is where the reference accelerometers are located.

555 Setting up the sensors for each swipe took in the region of 35-45 minutes and during each swipe  
 556 acceleration was recorded for 24 minutes. In an effort to minimise any time drift in the IMU signals,  
 557 just before the start of each swipe the five IMUs used in the test were brought together for at least  
 558 two minutes to allow mesh synchronisation to occur, then they would be distributed to the test  
 559 points for that swipe. Carrying out the test this way ensured that at least at the start of every swipe  
 560 the IMUs were synchronised. The observed performance of the IMU's with respect to time drift is  
 561 discussed in detail in the next section. For ease of cabling the logging station was set up on the 3<sup>rd</sup>  
 562 floor and is shown in Fig. 13(b).

563 The fact that the QAs need a logging station means that cables need to be ran through peoples'  
 564 offices and more problematically through public corridors and stairwells, to get the accelerometer  
 565 signals to the logging station. Aside from the time it takes to, (a) install the cables, (b) secure them to  
 566 minimise the trip hazard, and (c) remove them after the test. A significantly larger amount of time is  
 567 spent preparing Health and Safety method statements and agreeing with the building operator safe  
 568 routes for the cabling etc. For the IMUs (a)-(c) are simply not necessary, and as a result the time  
 569 required to prepare and agree the method statements and risk assessments for a purely IMU test  
 570 would only be a fraction of the time for the corresponding wired test.

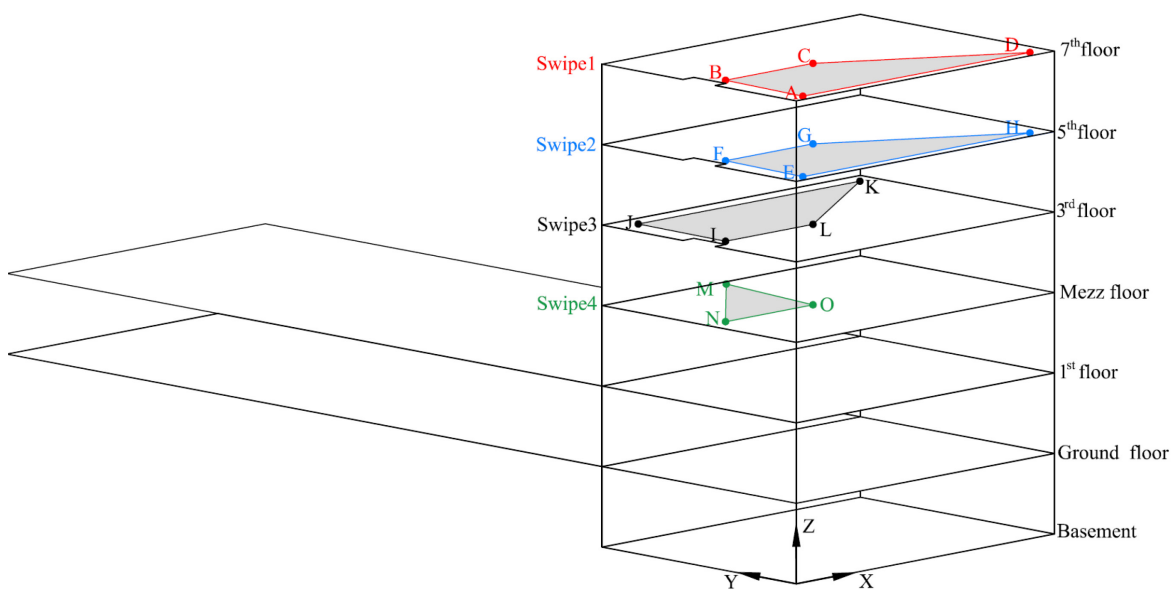
571 Table 3, Test points in each of the four swipes

Swipe No	Floor where most of the Test points are	Test points in the swipe*
1	7 <sup>th</sup> floor	<b>A</b> , B, C, D
2	5 <sup>th</sup> floor	<b>A</b> , E, F, G, H
3	3 <sup>rd</sup> floor	<b>A</b> , I, J, K, L
4	Mezzanine floor	<b>A</b> , M, N, O

*\*Test point where reference accelerometers located is indicated in bold*

572

573



574

575 Fig. 12, 3D schematic of the tower with the test points on each floor indicated.



(a)



(b)

576 Fig. 13, (a) two QA accelerometers and one IMU sensor at test point A on the 7<sup>th</sup> floor (b) data  
577 acquisition

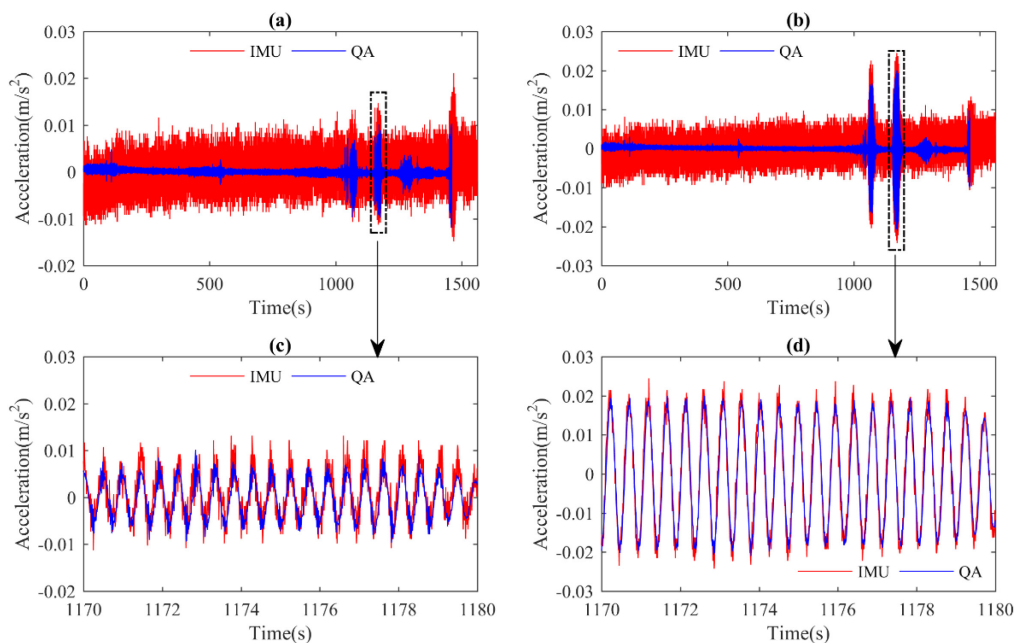
578 Fig. 14 shows the signals recorded at test point A (the reference location on the 7<sup>th</sup> floor) during  
579 swipe 1, with parts (a) and (b) showing the acceleration in the x and y directions respectively. The  
580 first thing to notice about Figs. 14 (a) and (b) is that the noise floor for the QA's is much lower than  
581 for the IMUs, reflecting the result shown in Fig. 2. On the night of the test there was almost no wind  
582 so the tower was moving very little and as a result in the first 750 seconds (i.e. the first half) of the  
583 swipe the IMU signal is essentially just noise. However, the noise floor of the QA accelerometer is  
584 sufficiently low that it is picking up the tower vibrations. The difference in the performance of the  
585 both sensors in the first 750 seconds can be seen more clearly in the frequency domain. Figs. 15 (i) &  
586 (ii) respectively show the result of analysing the first 750 seconds of the signals shown in Figs. 14 (a)  
587 & (b) with the Welch method, window lengths of 120 seconds with a 50% overlap were used. It can  
588 be seen in Figs. 15 (i) & (ii) that the QA's are identifying frequencies of 2.5 Hz and 2.1 Hz in the x and  
589 y directions respectively but that the IMU is not capturing these frequencies.

590 In an attempt to excite the tower sufficiently that the magnitude of the vibrations would be above  
591 noise floor of the IMUs it was decided to try excite the structure with three people stepping laterally  
592 from foot to foot at the building frequency. To excite a lateral frequency of 2.1 Hz required the  
593 authors to step laterally at a rate of 4.2 steps per second. To achieve this rhythm an audio  
594 metronome was set to 252 beats per minute and the three authors stepped/jumped at this rate on  
595 the 7<sup>th</sup> floor of the building. Fig. 16 shows an image of the authors jumping, note in this image the  
596 authors shoulders are parallel with the y axis of the building. The large pulses in acceleration at  
597 approximately 1100 seconds in Fig. 14 (a) & (b) are as a result of this jumping. The zoomed in view  
598 shown in Fig. 14 (c) & (d) shows clear sinusoidal signals for both the IMUs and QAs and it can be seen  
599 that the signals from the IMUs agree very well with the signals from the QA's.

600 Once the 2.1 Hz mode had been excited the authors realigned so that they were standing one  
601 behind the other but now their shoulders were parallel with the buildings x axis. To excite a

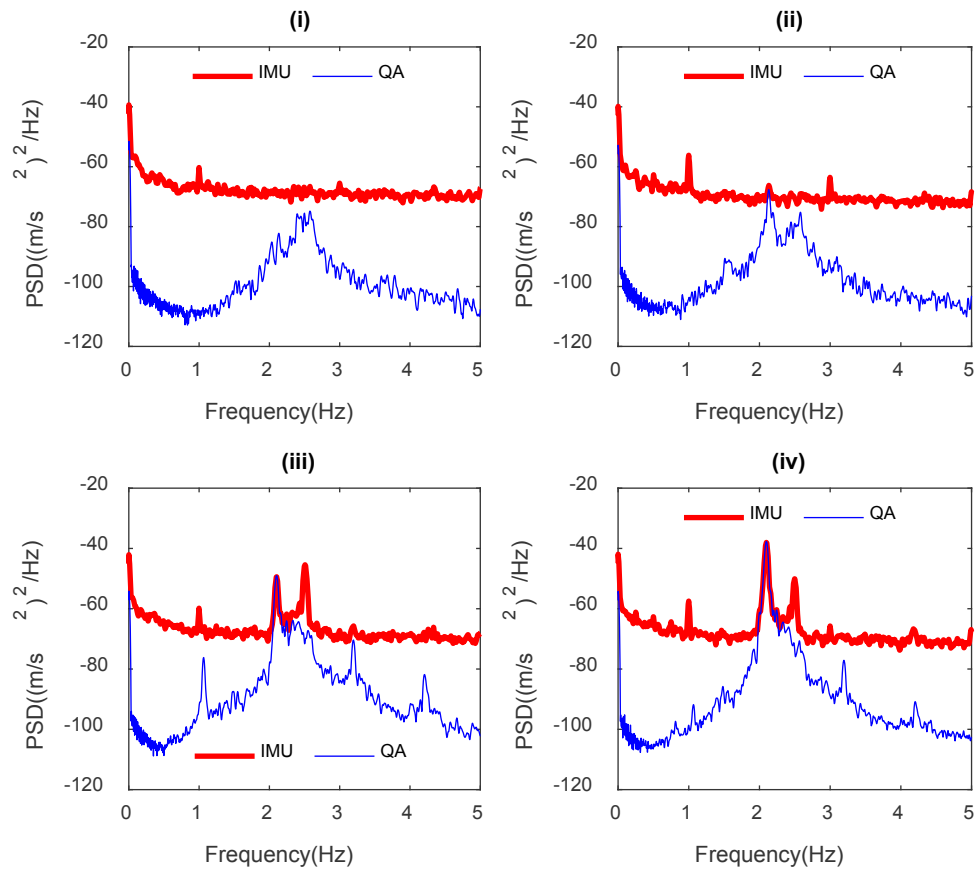
602 frequency of 2.5 Hz required the authors to step at a rate of 5 steps per second. The pulses in IMU  
 603 acceleration visible in Fig. 14 (a) & (b) at approximately 1400 seconds are as a result of this  
 604 stepping/jumping. However, it should be noted that the authors found 5 steps per second towards  
 605 the upper end of what was physically possible and it would be impossible to excite higher modes  
 606 using this technique. The reason the IMU time series in Fig. 14(a) and Fig. 14(b) is a little longer than  
 607 the QA time series is that the data logger recording the QA signals had been programmed to  
 608 automatically stop recording after 24 minutes, so the QAs just missed the jumping/stepping in the x-  
 609 direction.

610 Figs. 15(iii) and (iv) respectively show the frequency content of the signals that were recorded during  
 611 the jumping phase of the test, i.e. the signals in the latter half of Fig. 14(a) and (b), from 750 seconds  
 612 onwards. Unlike Figs. 15(i) and (ii) when the IMU data were unable to capture the building  
 613 frequencies in Figs. 15(iii) and (iv), the building frequencies are clearly evident in the IMU data. Once  
 614 it had been shown that the IMUs could capture the tower frequencies provided the building was  
 615 excited by humans jumping this procedure was also followed for Swipes 2-4. At the end of each  
 616 swipe all five IMUs were brought together to allow them to resynchronise if they had lost  
 617 synchronisation. The mode shapes identified from both the QA and IMU data are presented in  
 618 section 5.4.



619  
 620 Fig. 14 Acceleration recorded at reference location (test point A) during swipe 1, (a) acceleration in  
 621 x-direction (b) acceleration in y-direction, (c) zoomed in in view at 1170 seconds (d) zoomed in in  
 622 view at 1170 seconds

623



624

625 Fig. 15, Frequency content of the signals shown in Fig. 14, (i) frequency content of the first 750  
 626 seconds of acceleration data shown in Fig. 14(a), (ii) frequency content of the first 750 seconds of  
 627 acceleration data shown in Fig. 14(b), (iii) frequency content of second half of the IMU acceleration  
 628 signal shown in Fig. 14(a) i.e. after 750 seconds, (iv) frequency content of second half of the IMU  
 629 acceleration signal shown in Fig. 14(b) i.e. after 750 seconds.

630



631

632 Fig. 16, three of the authors stepping laterally to a predetermined beat on the 7<sup>th</sup> floor to excite  
633 building motion.

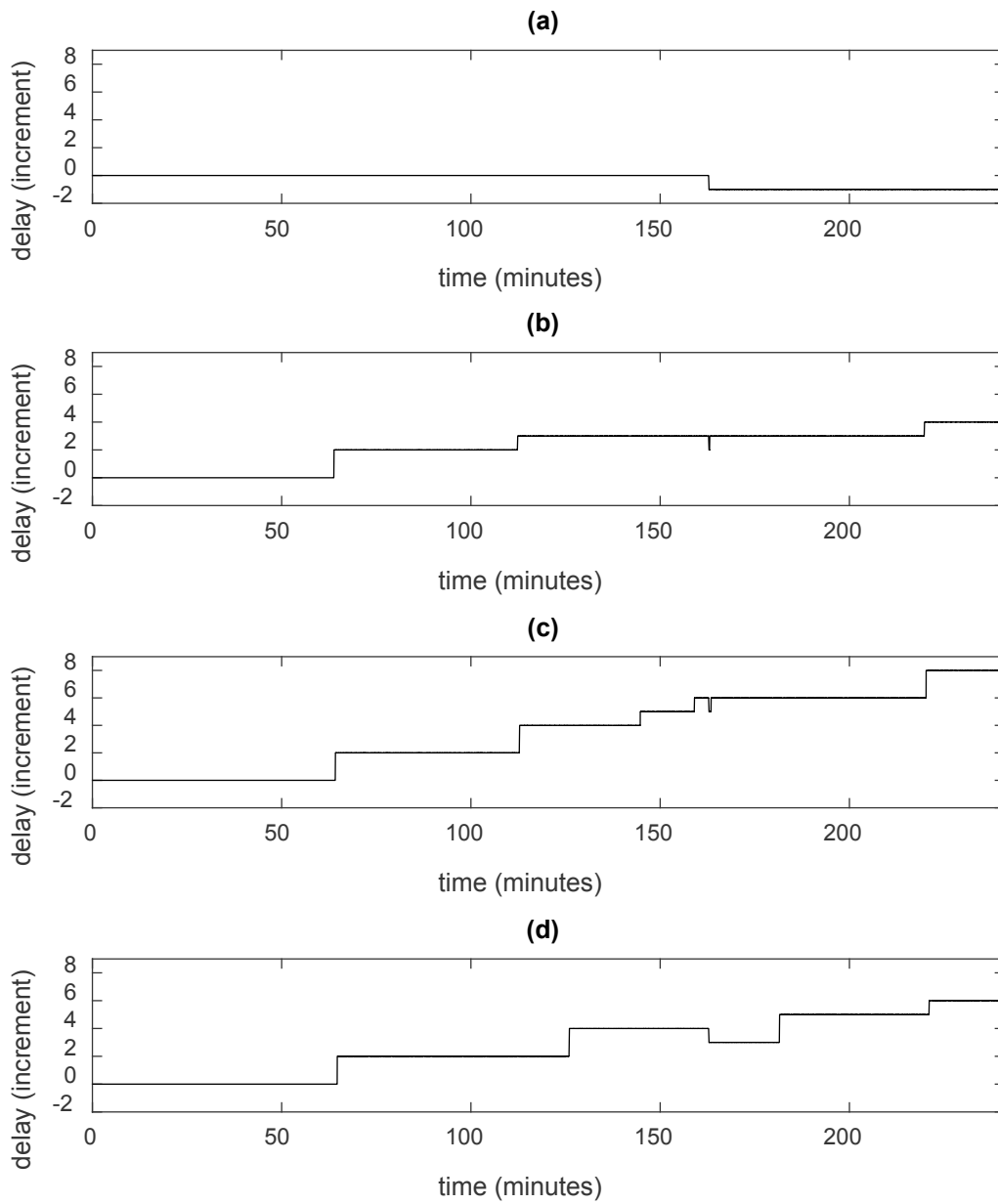
634

### 635 5.3 IMU Synchronisation

636 Prior to carrying out modal identification on the tower data, the amount of time drift that occurred  
637 between the different IMUs was investigated. As explained in Section 2.2 each IMU has its own  
638 internal clock and the data recorded at a given time instant is time stamped against the time on the  
639 internal clock. When operating in SLM, if the IMUs remain within range of each other the timing of  
640 each internal clock is adjusted according to a probabilistic model, so the time on all the clocks  
641 remains identical and therefore the data from each IMU is synchronised. Once an individual IMU  
642 sensor is out of range of its companions in the network, then the clock in that IMU is running  
643 independently so there is a possibility that it will start to run slightly ahead, or slightly behind the  
644 internal clocks of the other IMUs. The likelihood of the clock of the isolated IMU starting to run  
645 slightly ahead/behind the clocks of the other IMUs is increased if the isolated sensor is placed in a  
646 significantly different temperature to the other IMUs in the network. Once all the IMUs are reunited,  
647 i.e. that all five are within wireless range of each other, the probabilistic timing model will engage  
648 and identify what it considers the 'correct' time. Then the clock of any IMU not reading the correct  
649 time will be adjusted forwards or backwards such that it is reading the correct time. This occasional  
650 correcting of the time on the internal clock can be seen in post processing by examining the time  
651 stamps from the IMUs. The IMUs were scanning at 128 Hz so consecutive clock readings increase by  
652 0.0078125 seconds, henceforth known as one time increment. However, if the clock in an isolated  
653 IMU has started to run a little 'slow', when the isolated IMU is brought back to the rest of the  
654 network it's clock will increment by two (or possibly three) time increments in a single step to bring  
655 that clock into line with the other clocks in the network. Alternatively if the clock in the isolated IMU  
656 had started to run 'fast', when it is reunited with its companions in the network the timestamp may  
657 increment by zero between consecutive steps, or possibly even show a negative increase if it is two  
658 or more time increments out of synchronisation.

659 While the procedure described above (i.e. looking at the time stamps of individual IMUs) can be  
660 used to identify potential drift. When dealing with a network of five IMUs it is more meaningful to  
661 take the time stamp from one IMU as the reference, and compare the timestamps of the other four  
662 IMUs to the reference timestamp. Fig. 17 shows the result of carrying out such an exercise. IMU No  
663 5 was taken as the reference and its timestamp was compared to the timestamps of IMUs No's 1-4  
664 and the result of this comparison is shown in Figs. 17(a-d) respectively. It should be noted that the  
665 IMUs were recording from the start of the test until the end, i.e. IMU recording is not stopped  
666 between swipes, instead the swipe data (for the four individual swipes) is cut from the total IMU  
667 time series in post processing. In Fig 17(a) it can be seen that in total the IMUs were recording for  
668 approximately 240 minutes and that in this period IMU No 1 only drifted from IMU No 5 by one time  
669 increment and this occurred after 163 minutes. Parts (b), (c) and (d) of the figure also show some  
670 drift at 163 minutes. As described in section 5.2, all five IMUs are all together at the start of a swipe  
671 for at least two minutes, and the steps/drifts apparent at 163 minutes is evidence of the  
672 probabilistic timing model 'correcting' the time on the internal clocks when the IMUs are reunited  
673 after a period of separation for one or more of the IMUs. Other occasions where a step change is  
674 observed in the timing of multiple sensors occur at 64 minutes and 112 minutes. Each of the swipes  
675 were 24 minutes long, and it can be seen from Fig. 17 that in any given 24 minute period there is  
676 never more than two increment drift in the internal clocks of the IMUs. This equates to a maximum  
677 drift of approximately 0.0156 seconds ( $2 * 0.0078125 \approx 0.0156$ ). When one is dealing with frequencies  
678 less than 10Hz (period  $\geq 0.1$  seconds) even if an individual IMU goes out of synchronisation with the  
679 other sensors in the network by one time step (0.0078 s) or even two time steps (0.0156 s) over the  
680 course of a 24 minute swipe it effects the phase very little and as a result the mode shapes will still  
681 be correct. The timestamps of the individual IMUs were also checked after the modal test on the  
682 bridge (Section 4) however, for the bridge test there were zero slips evident. This is believed to be  
683 due to the fact that during the bridge test the IMUs were sufficiently close together to maintain  
684 mesh synchronisation in SLM for the duration of the bridge test.

685



688 Fig. 17 Variation between the internal clock of the reference IMU (IMU No 5) and the internal clocks  
689 of the other four IMUs in the network (a) Difference between the reference clock and IMU No 1, (b)  
690 Difference between the reference clock and IMU No 2, (c) Difference between the reference clock  
691 and IMU No 3, (d) Difference between the reference clock and IMU No 4.

695 5.4 Mode shapes from tower

696 Having satisfied ourselves that synchronisation will not be a significant problem, the modal  
697 identification procedure described in section 3.2.2 was implemented to identify the mode shapes  
698 from both the QA and IMU data and the results are shown in Table 4. The stick model in Table 4 can  
699 be understood if the sensor layout in Fig. 12 is examined. For modes 1 and 2 the mode shapes and  
700 frequencies calculated using the IMU sensors compare very well with those calculated using the  
701 wired QA system. However, mode shape 3 is not correctly identified from the IMU data. This may  
702 have been because the amplitudes of vibration associated with the third mode were simply so small  
703 that they were not detected properly by the accelerometer in the IMU, or it may be that for higher  
704 frequencies and therefore lower periods of vibration are more sensitive to time drift between  
705 individual IMUs if mesh synchronisation is lost during the swipe. However, the fact that modes 1 and  
706 2 are identified correctly in the IMU data is relatively impressive for two reasons. Firstly even with  
707 the jumping the magnitude of the acceleration was still quite small with the maximum amplitudes  
708 on the 7<sup>th</sup> floor in the region of 0.01 - 0.02 m/s<sup>2</sup> with even smaller amplitudes on the lower floors.  
709 Secondly for swipes 2-4 there were significant distances and obstructions between the IMUs on the  
710 floor being measured and the reference IMU on the 7<sup>th</sup> floor.

711 It is important to note that without having the QAs on site the night of the test it would have been  
712 very difficult for the authors to know what frequencies to jump at to excite the structure. If the  
713 authors only had IMU's on the night they would have had to jump at a series of different frequencies  
714 in the range of frequencies expected for the building, to see which provide the best excitation and  
715 this would have been very slow. However, as noted earlier on the night of the test the weather was  
716 extremely calm so a small follow up test was carried out on a windy night to see if the IMUs could  
717 capture the structural frequencies (without anyone jumping), and the results of this test are briefly  
718 reported in the next section.

719

720

721

722

723

724

725

726

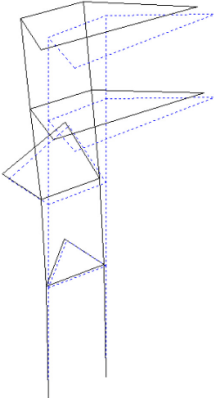
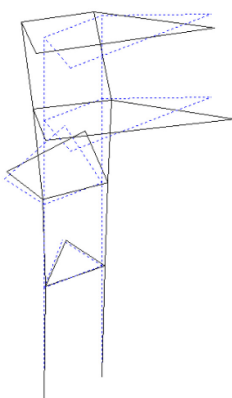
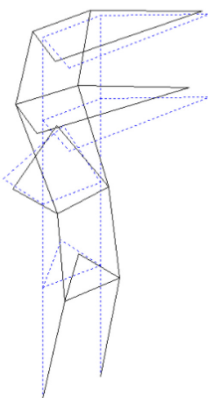
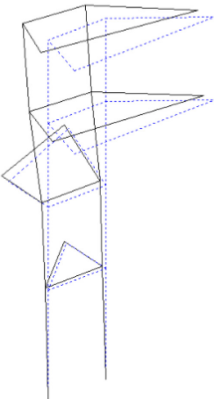
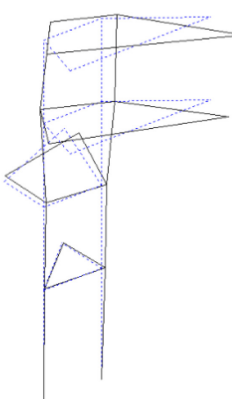
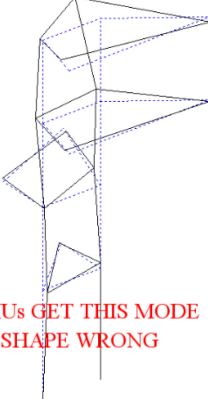
727

728

729

730

731 Table 4, Frequencies, damping coefficients and mode shapes for the first 3 tower modes

	Mode 1	Mode 2	Mode 3
QA	<p>Freq=2.11 Hz</p>  <p>Damping=0.44%</p>	<p>Freq=2.5 Hz</p>  <p>Damping=0.68%</p>	<p>Freq=10.8 Hz</p>  <p>Damping=0.071%</p>
IMU	<p>Freq=2.11 Hz</p>  <p>Damping=0.3%</p>	<p>Freq=2.52 Hz</p>  <p>Damping=0.4%</p>	<p>Freq=10.7 Hz</p>  <p>IMUs GET THIS MODE SHAPE WRONG</p> <p>Damping=0.51%</p>
	<b>0%</b> difference between IMU and QA Frequency	<b>0.79%</b> difference between IMU and QA Frequency	<b>0.93%</b> difference between IMU and QA Frequency

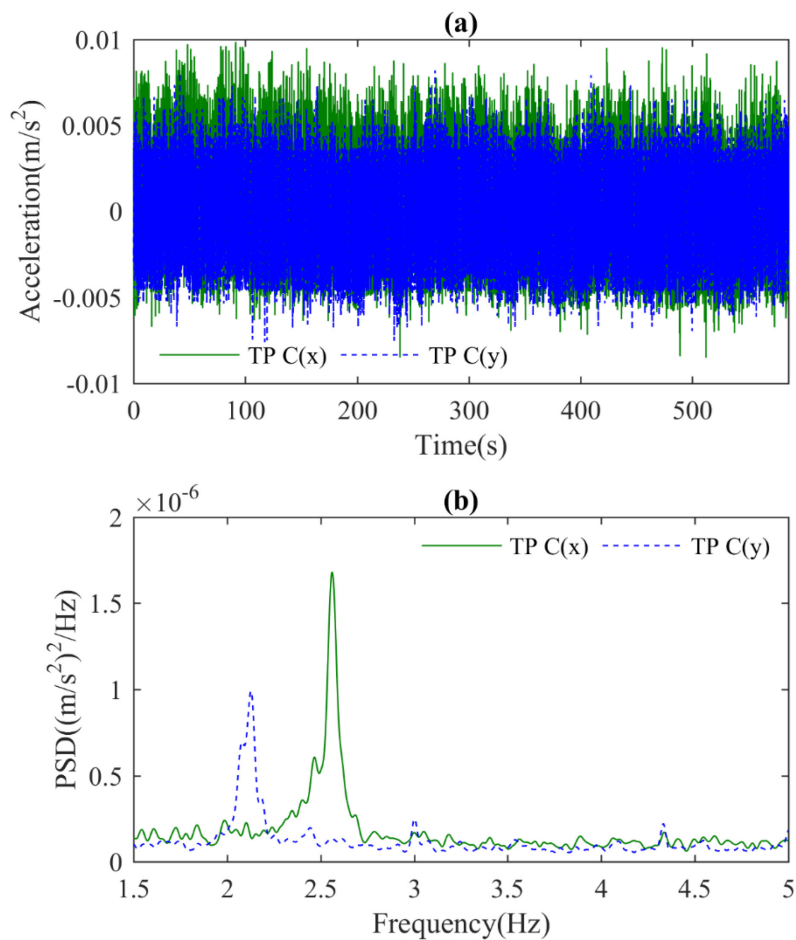
732

733

734 5.5 Limited testing on windy night

735 To see if the IMUs might be able to pick up the building frequencies without people jumping, a  
 736 limited test with just one IMU was carried out on a night with winds of approximately 20 mph. The  
 737 IMU was positioned on the 7<sup>th</sup> floor at test point C indicated in Fig. 11(a). Fig. 18(a) shows the  
 738 acceleration recorded in the x and y directions as solid and dashed plots respectively. Fig. 18(b)  
 739 shows the frequency content of the signals between 1.5 and 5 Hz and it can be seen that the  
 740 structural frequencies at 2.1 and 2.5 Hz are clearly visible. Therefore when there is sufficient wind to  
 741 excite the structure the IMUs are able to pick up the building frequencies without specific human  
 742 excitation.

743



744

745 Fig. 18, Data recorded at test point C on the 7<sup>th</sup> floor on a night when there was 20 mph wind (a)  
 746 time series data, (b) frequency content of acceleration data shown in (a).

747 **6.0 Discussion and conclusions**

748 In this study it was found that the mode shapes identified for the three structures using IMU  
 749 acceleration data, were very similar to the corresponding mode shapes identified from the QA  
 750 acceleration data. Admittedly for the modal test of the concrete office tower there were some  
 751 instances where the QAs were superior but these aspects are further discussed below.

752

753 For the floor structure in the laboratory the IMUs were never more than a few meters apart so no  
 754 problems with synchronisation were envisaged and indeed this proved to be the case as the IMUs  
 755 performed just as well as the QAs. In the laboratory there was ready availability of power, the  
 756 logging station could be set up wherever was convenient and there was no restrictions on where  
 757 cables could be ran. Therefore while the IMUs were still quicker to set up than the QAs the  
 758 difference was not that pronounced and any time advantages for the IMUs in the set up were at  
 759 least partially offset by the extra time required in post processing to cut the data for the 12 swipes  
 760 from the total IMU time record.

761

762 However, the test on the steel road bridge really highlighted the potential benefits of the IMUs. Two

763 of the basic requirements when setting up a logging station are electrical power and shelter from the  
764 elements. Unlike in a building where these things are readily available, on a bridge site these need to  
765 be provided/installed and this takes significant time. Installing the necessary cabling also takes a  
766 significant amount of time for three principle reasons;

767 (i) bridge remaining open: during a modal test on a bridge, the bridge will normally remain open to  
768 vehicle and pedestrian traffic which places limitations on where cables can be placed, thereby  
769 forcing the tester to position the cables in zones with more difficult access, which slows the process  
770 down,

771 (ii) length of cable required: the physical size of a real bridge means that tens to hundreds of meters  
772 of cable need to be installed,

773 (iii) challenging access: depending on the height of the deck, what passage the bridge is crossing,  
774 limited access to abutments, revetments etc. means it can be difficult/slow to get to the places  
775 cables need to be installed.

776 As a result planning and executing the wired test took over one hundred man hours, gathering the  
777 same information with the IMUs took approximately ten man hours. After processing the data, the  
778 mode shapes from the IMU data were the same as the mode shapes from the QA data. This shows  
779 that for the bridge tested the accelerometers in the IMUs were sensitive enough to accurately  
780 capture the vibrations and that synchronisation between the IMUs was adequate.

781

782 The structure where the IMUs struggled a bit was the tower. Prior to the tower test the authors'  
783 primary concern was that in the tower, the IMUs would not have clear lines of sight between each  
784 other for wireless communication and therefore one or more sensors might drift (in time)  
785 significantly from the others and as a result the IMUs' signals might not be time synchronised.  
786 However, this did not prove to be such an issue. Instead it was found that for very low levels of  
787 vibration the noise floor in the IMUs accelerometer is simply too high to allow accelerations to be  
788 identified so it was necessary for the authors to artificially induce acceleration at a level high  
789 enough for the IMUs to detect it. If the test had been carried out on a windy night it appears from  
790 section 5.5 that the IMUs would not need human induced vibrations as the wind is sufficient to  
791 excite the structure. Essentially the tower test showed that the primary limitation of the IMUs for  
792 structural modal testing is the quality of the accelerometer rather than issues with synchronisation.

793

794 From the three structures tested it was shown that over the course of a 20-30 minute swipe  
795 (commonly used for a modal test on a structure) the IMUs did not drift significantly in time. This  
796 means that if a more sensitive accelerometer was used they really could be very useful for structural  
797 modal testing, particularly on bridge sites. However, if one was going to change the accelerometer it  
798 would make sense to make the units a little bigger, and install the hardware necessary to increase  
799 the range of the wireless capabilities so that the sensors could remain in wireless communication  
800 over longer distances and therefore remain mesh synchronised.

801

802 **Acknowledgements**

803 The research leading to these results has received funding from the People Programme (Marie Curie  
804 Actions) of the European Union's Seventh Framework Programme (FP7/2007-2013) under grant  
805 agreement n° 330195. The authors would also like to acknowledge the Bridge Section of The  
806 Engineering Design Group of Devon County Council led by Kevin Dentith BSc, CEng, FICE, for their  
807 support and assistance with this work.

808 **References**

- 809 [1] P. Moyo, J.M.W. Brownjohn, P. Omenzetter, Highway bridge live loading assessment and load  
810 carrying estimation using a health monitoring system, *Struct. Eng. Mech.* 18 (2004) 609–626.
- 811 [2] F.N. Catbas, T. Correa-Kijewski, A.E. Aktan, *Structural Identification of Constructed Systems.*  
812 *Approaches, Methods and Technologies for Effective Practice of St-Id.*, ASCE, 2013.
- 813 [3] S. Jang, H. Jo, S. Cho, K. Mechitov, J. a Rice, S.H. Sim, H.J. Jung, C.B. Yun, B.F. Spencer, G. Agha,  
814 *Structural health monitoring of a cable-stayed bridge using smart sensor technology:*  
815 *deployment and evaluation*, *Smart Struct. Syst.* 6 (2010) 439–459.  
816 doi:10.12989/sss.2010.6.5\_6.439.
- 817 [4] S. Jang, S.-H. Sim, H. Jo, B.F. Spencer Jr, Full-scale experimental validation of decentralized  
818 damage identification using wireless smart sensors, *Smart Mater. Struct.* 21 (2012) 115019.  
819 doi:10.1088/0964-1726/21/11/115019.
- 820 [5] G.L. Smidt, R.H. Deusinger, J. Arora, J.P. Albright, An automated accelerometry system for gait  
821 analysis, *J. Biomech.* 10 (1977) 367–375. doi:10.1016/0021-9290(77)90009-4.
- 822 [6] H.J. Luinge, P.H. Veltink, Measuring orientation of human body segments using miniature  
823 gyroscopes and accelerometers, *Med. Biol. Eng. Comput.* 43 (2005) 273–282.  
824 doi:10.1007/BF02345966.
- 825 [7] F. Brunetti, J.C. Moreno, A.F. Ruiz, E. Rocon, J.L. Pons, A new platform based on IEEE802.15.4  
826 wireless inertial sensors for motion caption and assessment, in: *Int. Conf. IEEE Eng. Med. Biol.*  
827 *Soc.*, 2006: pp. 6497–6500.
- 828 [8] M. Bocian, J.M.W. Brownjohn, V. Racic, D. Hester, A. Quattrone, R. Monnickendam, A  
829 framework for experimental determination of localised vertical pedestrian forces on full-scale  
830 structures using wireless attitude and heading reference systems, *J. Sound Vib.* 376 (2016)  
831 217–243. doi:10.1016/j.jsv.2016.05.010.
- 832 [9] B. Peeters, W. Hendricx, J. Debille, Modern Solutions for Ground Vibration Testing of Large  
833 Aircraft, *Sound Vib.* 295 (2009) 8–15. doi:10.4271/2008-01-2270.
- 834 [10] A. Pavic, Z. Miskovic, P. Reynolds, Modal Testing and Finite-Element Model Updating of a  
835 Lively Open-Plan Composite Building Floor, *J. Struct. Eng.* 133 (2007) 550–558.  
836 doi:10.1061/(ASCE)0733-9445(2007)133:4(550).
- 837 [11] D.J. Ewins, *Modal Testing: Theory, Practice and Application*, Research Studies Press Ltd.,  
838 Baldock, Hertfordshire, England, 2000.
- 839 [12] A.M. Abdel-Ghaffar, R.H. Scanlan, Ambient vibration studies of Golden Gate bridge: 1.  
840 Suspended structure, and 2. Pier tower structure, *ASCE J. Eng. Mech.* 111 (1985) 463–482.  
841 doi:10.1061/(ASCE)0733-9399(1985)111:4(463).

- 842 [13] J.M.W. Brownjohn, E.P. Carden, C.R. Goddard, G. Oudin, Real-time performance monitoring  
843 of tuned mass damper system for a 183m reinforced concrete chimney, *J. Wind Eng. Ind.*  
844 *Aerodyn.* 98 (2010) 169–179. doi:10.1016/j.jweia.2009.10.013.
- 845 [14] S.K. Au, Uncertainty law in ambient modal identification---Part II: Implication and field  
846 verification, *Mech. Syst. Signal Process.* 48 (2014) 34–48. doi:10.1016/j.ymsp.2013.07.017.
- 847 [15] PCB Piezotronics, PCB Piezotronics, (2017). <http://www.pcb.com/Products/model/393c>  
848 (accessed October 8, 2017).
- 849 [16] Honeywell, Q-Flex QA-750, (2017).  
850 [https://aerospace.honeywell.com/en/~media/aerospace/files/brochures/accelerometers/q-](https://aerospace.honeywell.com/en/~media/aerospace/files/brochures/accelerometers/q-flexqa-750accelerometer_bro.pdf)  
851 [flexqa-750accelerometer\\_bro.pdf](https://aerospace.honeywell.com/en/~media/aerospace/files/brochures/accelerometers/q-flexqa-750accelerometer_bro.pdf) (accessed October 8, 2017).
- 852 [17] Kinometrics, Episensor, (2017). [https://kinometrics.com/post\\_products/episensor-es-t/](https://kinometrics.com/post_products/episensor-es-t/)  
853 (accessed October 8, 2017).
- 854 [18] L. Nachman, J. Huang, J. Shahabdeen, R. Adler, R. Kling, IMOTE2: Serious computation at the  
855 edge, *Proc. IWCMC 2008 - Int. Wirel. Commun. Mob. Comput. Conf.* (2008) 1118–1123.
- 856 [19] J. a. Rice, B.F. Spencer, Jr., Structural health monitoring sensor development for the Imote2  
857 platform, *Proc. SPIE - Int. Soc. Opt. Eng.* 6932 (2008) 693231–693234.  
858 doi:10.1117/12.776695.
- 859 [20] M. Kane, D. Zhu, M. Hirose, X. Dong, B. Winter, M. Häckell, J.P. Lynch, Y. Wang, A. Swartz,  
860 Development of an extensible dual-core wireless sensing node for cyber-physical systems, in:  
861 *SPIE - Int. Soc. Opt. Eng.*, 2014: p. 90611U. doi:10.1117/12.2045325.
- 862 [21] S. Cho, H. Jo, S. Jang, J. Park, H.J. Jung, C.B. Yun, B.F. Spencer, J.W. Seo, Structural health  
863 monitoring of a cable-stayed bridge using wireless smart sensor technology: data analyses,  
864 *Smart Struct. Syst.* 6 (2010) 461–480.
- 865 [22] D. Zhu, Y. Wang, J.M.W. Brownjohn, Vibration testing of a steel girder bridge using cabled and  
866 wireless sensors, *Front. Archit. Civ. Eng. China.* 5 (2011) 249–258. doi:10.1007/s11709-011-  
867 0113-y.
- 868 [23] J. Li, T. Nagayama, K.A. Mechitov, B.F. Spencer, Efficient campaign-type structural health  
869 monitoring using wireless smart sensors, in: *Proc. SPIE - Sensors Smart Struct. Technol. Civil,*  
870 *Mech. Aerosp. Syst.*, 2012: p. 83450U–83450U–11. doi:10.1117/12.914860.
- 871 [24] J.M.W. Brownjohn, F. Magalhães, E. Caetano, A. Cunha, Ambient vibration re-testing and  
872 operational modal analysis of the Humber Bridge, *Eng. Struct.* 32 (2010) 2003–2018.  
873 doi:10.1016/j.engstruct.2010.02.034.
- 874 [25] Guralp, MAN-RTM-0003 - Real-time Clock Operator's Guide, (2016).
- 875 [26] J.M.W. Brownjohn, S.K. Au, B. Li, J. Bassitt, Optimised ambient vibration testing of long span  
876 bridges, in: *EURODYN 2017, 2017*: p. 10. doi:10.1016/j.proeng.2017.09.147.
- 877 [27] Y.L. Xi, Y.C. Zhu, S.K. Au, Operational modal analysis of Brodie Tower using a Bayesian  
878 approach, in: *UNCECOMP 2017 Int. Conf. Uncertain. Quantif. Comput. Sci. Eng.*, 2017: p. 10.
- 879 [28] K.Y. Wong, K.W.Y. Chan, K.L. Man, Monitoring of wind load and response for cable-supported  
880 bridges in Hong Kong, in: *Proc SPIE 4337, Heal. Monit. Manag. Civ. Infrastruct. Syst.*, 2001: p.  
881 12.

- 882 [29] K. Lebel, P. Boissy, M. Hamel, C. Duval, Inertial measures of motion for clinical biomechanics:  
883 Comparative assessment of accuracy under controlled conditions - Effect of velocity, PLoS  
884 One. (2013). doi:10.1371/journal.pone.0079945.
- 885 [30] V. Krishnamurthy, K. Fowler, E. Sazonov, The effect of time synchronization of wireless  
886 sensors on the modal analysis of structures, Smart Mater. Struct. 17 (2008) 055018.  
887 doi:10.1088/0964-1726/17/5/055018.
- 888 [31] J.M.W. Brownjohn, M. Bocian, D. Hester, A. Quattrone, W. Hudson, D. Moore, S. Goh, M.S.  
889 Lim, Footbridge system identification using wireless inertial measurement units for force and  
890 response measurements, J. Sound Vib. 384 (2016) 339–355. doi:10.1016/j.jsv.2016.08.008.
- 891 [32] R. Sleeman, Three-Channel Correlation Analysis: A New Technique to Measure Instrumental  
892 Noise of Digitizers and Seismic Sensors, Bull. Seismol. Soc. Am. 96 (2006) 258–271.  
893 doi:10.1785/0120050032.
- 894 [33] S.K. Au, J.M.W. Brownjohn, J.E. Mottershead, Quantifying and managing uncertainty in  
895 operational modal analysis, Mech. Syst. Signal Process. 102 (2018) 139–157.  
896 doi:10.1016/j.ymssp.2017.09.017.
- 897 [34] J.M. Caicedo, Practical guidelines for the natural excitation technique (NExT) and the  
898 eigensystem realization algorithm (ERA) for modal identification using ambient vibration, Exp.  
899 Tech. 35 (2011) 52–58. doi:10.1111/j.1747-1567.2010.00643.x.
- 900 [35] C. Gentile, N. Gallino, Ambient vibration testing and structural evaluation of an historic  
901 suspension footbridge, Adv. Eng. Softw. 39 (2008) 356–366.  
902 doi:10.1016/j.advengsoft.2007.01.001.
- 903 [36] K. Van Nimmen, P. Van den Broeck, P. Verbeke, C. Schauvliege, M. Malli?, L. Ney, G. De  
904 Roeck, Numerical and experimental analysis of the vibration serviceability of the Bears' Cage  
905 footbridge, Struct. Infrastruct. Eng. 13 (2017) 390–400. doi:10.1080/15732479.2016.1160133.
- 906 [37] S.K. Au, Operational Modal Analysis: Modeling, Bayesian Inference, Uncertainty Laws,  
907 Springer, 2017.
- 908 [38] J.M.W. Brownjohn, H. Hao, T.-C. Pan, Assessment of structural condition of bridges by  
909 dynamic measurements Applied Research Report RG5/97, (2001) -.
- 910 [39] J.N. Juang, R.S PAppa, An eigensystem realization algorithm for modal parameter  
911 identification and modal reduction, J. of Guidance, 8 (2015) 620-627
- 912 [40] G.H. James, T.G. Carne, J.P. Lauffer, The natural excitation technique (NExT) for modal  
913 parameter extraction from operating structures, Journal of analytical and Experimental modal  
914 analysis, 10 (1995) 260-277
- 915 [41] P.D. Welch, The use of fast Fourier transform for the estimation of power spectra: A method  
916 based on time averaging over short, modified periodograms, IEEE Trans. Audio Electroacoust.  
917 15 (1967) 70–73.
- 918 [42] H. Nandan, M.P. Singh, Effects of thermal environment on structural frequencies: Part I - A  
919 simulation study, Eng. Struct. 81 (2014) 480–490. doi:10.1016/j.engstruct.2014.06.046.

920

921